Journal of Solid State Chemistry **152,** 302–321 (2000)
doi:10.1006/jssc.2000.8676, available online at http://www.idealibrary.com on IDEAL®

Building Open-Framework Metal Phosphates from Amine Phosphates and a Monomeric Four-Membered Ring Phosphate

C. N. R. Rao,[1] Srinivasan Natarajan, and S. Neeraj

Chemistry and Physics of Materials Unit and CSIR Centre of Excellence in Chemistry, Jawaharlal Nehru Centre for Advanced Scientific Research, Jakkur P.O., Bangalore 560 064, India

Several amine phosphates have been synthesized and their structures elucidated by single crystal X-ray diffraction. The amine phosphates, on reaction with metal ions, give rise to a large variety of metal phosphate structures incorporating the amine molecules, thus providing a facile route to the open-framework materials. By means of such a soft chemical method, it has been possible to generate novel architectures, typical of these being a cloverite structure, a new chlorophosphate incorporating chlorine as part of the framework, and a four-membered ring monomeric phosphate. The studies indicate that amine phosphates are likely to act as intermediates in the formation of open-framework metal phosphates. The transformation of the monomeric zinc phosphate to an open-framework layered structure on heating it in water suggests the four-membered ring to be the basic building unit. © 2000 Academic Press

Key Words: **hydrothermal methods; intermediates; phosphates; open-framework structures.**

1. INTRODUCTION

Open-framework metal phosphates constitute an important family of materials obtained by hydrothermal synthesis in the presence of structure-directing organic amines (1). Particular interest in these materials arises because of the possibility of rendering them porous by the removal of the amine template just as in the case of aluminosilicates and other zeolitic materials (2). While the mode of formation of aluminosilicate structures is fairly well understood, we do not yet have a meaningful picture of the mechanism of formation of open-framework metal phosphate structures (3). The role of amine in the formation of the metal phosphates itself has not been unraveled. There has been some discussion as to the nature of the basic building block, which on condensation self-assembly gives rise to the more complex open-framework structures. Thus, Ferey (4) has proposed assemblies of metal–oxygen polyhedra and phosphate tetrahedra to constitute the basic building unit of open-framework metal phosphates. In the case of aluminophosphates, a linear chain has been suggested to be the basic building block (5). The linear chain itself consists of corner-shared four-membered rings and it is therefore important to explore whether the four-membered ring is the fundamental unit of the structures. We have been interested in understanding the formation of open-framework metal phosphates by exploring the mode of formation by different pathways. In this paper we describe the results of two types of experiments carried out by us. The first set of experiments pertains to the isolation of amine phosphate intermediates (6) and their further reaction with metal ions to form open-framework structures. The second type of effort involves the isolation of a four-membered ring monomer and its transformation to a complex open-framework architecture. Based on the present study, we propose pathways for the formation of open-framework metal phosphates starting from simple building units.

[1] To whom correspondence should be addressed. Fax: 91-80-846-2766. E-mail: cnrrao@jncasr.ac.in.

2. EXPERIMENTAL

2.1. Synthesis of Amine Phosphates

It has been known that during hydrothermal synthesis of open-framework metal phosphates, amine phosphates appear as unwanted side products (7). Not much attention, however, has been paid to the study of amine phosphates and their role in the formation of metal phosphates. In order to probe the formation of metal phosphates, we sought to synthesize a large number of amine phosphates. The amine phosphates are, in general, prepared by the dropwise addition of the amine to an aqueous/methanolic solution of phosphoric acid under continuous stirring. The resulting gel is allowed to stand at room temperature; in some cases hydrothermal processing in a sealed polypropylene bottle is also carried out (see Table 1), followed by cooling to room temperature to yield the desired crystals. In a typical experiment for the synthesis of 1,4-diazabicyclo[2,2,2]octane

0022-4596/00 $35.00

TABLE 1
Conditions Employed for the Synthesis of Amine Phosphates

Code	Gel composition	T (K)	t (h)	Product composition
PIPP	$1.0C_4N_2H_{10}:1.2H_3PO_4:5.5H_2O$	383	10	$(C_4N_2H_{12})(HPO_4).H_2O$
MPIP-P[a,b]	$1.0C_5N_2H_{12}:1.2H_3PO_4:5.5H_2O$	383	10	$(C_5N_2H_{14})_2(HPO_4)_2.3H_2O$
DETAP	$1.0C_4N_3H_{13}:1.2H_3PO_4:5.5H_2O$	383	10	$(C_4N_3H_{15})(HPO_4)_2(H_2O)$
DABCO-P[a,b]	$1.0C_6N_2H_{12}:1.2H_3PO_4:5.5H_2O$	383	10	$(C_6N_2H_{14})(HPO_4).H_2O$
1,2-DAPP[a]	$1.0C_3N_2H_{10}:1.2H_3PO_4:5.5H_2O$	383	10	$(C_3N_2H_{12})(HPO_4)$
ENP	$1.0C_2N_2H_8:1.2H_3PO_4:5.5H_2O$	383	10	$(C_2N_2H_{10})(HPO_4)$
DAHP[a]	$1.0C_6N_2H_{16}:1.2H_3PO_4:5.5H_2O$	383	10	$(C_6N_2H_{18})_3(HPO_4)_3.4H_2O$
APPIP-P[a,b]	$1.0C_{10}N_4H_{24}:1.2H_3PO_4:50MeOH$	353	2	$(C_{10}N_4H_{26})(HPO_4).2H_2O$
1,3-DAPP	$1.0C_3N_2H_{10}:1.2H_3PO_4:5.5H_2O$	383	10	$(C_3N_2H_{12})(HPO_4).H_2O$
TMED-P[a,b]	$1.0C_6N_2H_{16}:1.2H_3PO_4:50MeOH$	353	2	$(C_6N_2H_{18})(HPO_4).2H_2O$

[a] New amine phosphates.
[b] Described in the present study.

(DABCO) phosphate, (DABCO-P), 10 mM DABCO was dissolved in 50 mM of water. To this mixture 12 mM of H_3PO_4 (aq. 85 wt%) was added dropwise and stirred. The resultant gel, with a final composition of DABCO : 1.2 H_3PO_4 : $5H_2O$, was sealed in a polypropylene bottle and heated at 110°C for 6 h. The mixture, after the above heat treatment, was poured in to a 25-ml beaker and left to crystallize at room temperature. Large, colorless, transparent, plate-like crystals resulted from the mixture after ~24 h. The various amine phosphates that have been synthesized and characterized in the present study are listed in Table 1. The amine phosphates, thus prepared, were characterized using conventional chemical techniques, such as chemical analysis and thermogravimetry (TGA). In addition, single crystal X-ray diffraction was used to determine the structure in select cases. The cell parameters for the various amine phosphates are presented in Table 2. While a few of them were reported earlier in the literature, several are new.

TABLE 2
Crystallographic Parameters for the Amine Phosphates

	Cell parameters							
Code	a (Å)	b (Å)	c (Å)	α (°)	β (°)	γ (°)	Sp. grp.	Ref.
PIPP	6.426	12.297	11.221	90.0	97.1	90.0	$P2_1/n$	[7]
MPIP-P	12.163	6.776	25.740	90.0	103.3	90.0	$P2_1/n$	[a]
DETAP	6.116	10.667	17.061	90.0	90.0	90.0	$P2_12_12_1$	[8]
DABCO-P	6.906	9.018	9.271	92.2	104.5	111.8	$P(-1)$	[a]
1,2-DAPP	10.869	6.278	11.389	90.0	104.5	90.0	$P2_1/n$	[a]
ENP	7.507	11.816	8.055	90.0	110.1	90.0	$P2_1/c$	[9]
DAHP	10.307	13.456	15.109	66.6	77.5	68.3	$P(-1)$	[a]
APPIP-P	6.608	8.571	10.130	112.4	96.6	102.6	$P(-1)$	[a]
1,3-DAPP	7.001	16.776	7.846	90.0	113.8	90.0	$P2_1/c$	[8]
TMED-P	8.209	8.412	8.618	114.3	94.9	118.1	$P(-1)$	[a]

[a] This work.

The synthesis of metal phosphates was carried out hydrothermally by the reaction between the amine phosphate and the appropriate metal ions under aqueous or nonaqueous conditions. The compositions and crystallographic parameters of the open-framework metal phosphates obtained from the reaction of amine phosphates with metal ions are presented in Table 3. Many of these metal phosphates are new as can be seen from Table 3, and several phosphates prepared by the conventional hydrothermal methods are produced alongside. Synthetic procedures of a few typical metal phosphates are described below.

2.2. Synthesis of Zinc Phosphate, **I**, *$[C_4N_2H_{12}]_{0.5}[Zn(HPO_4)(H_2PO_4)]$*

ZnO (1 mM) was dispersed in a mixture containing 80 mM of butan-2-ol and 20 mM of water. To this, 2 mM of HCl (35 wt%) was added to help the dissolution of the zinc oxide. *N*-methyl piperazine phosphate (MPIP-P) (2.6 mM) was added to the above mixture under continuous stirring. The final mixture was homogenized for 30 min, sealed in a 23-ml PTFE-lined stainless steel pressure vessel (Parr, Moline, USA), and heated at 170°C for 72 h. The product of the above reaction, containing a large quantity of colorless crystals, were filtered and washed with minimum quantity of water and dried under laboratory conditions.

2.3. Synthesis of Cobalt Phosphate, **II**, *$[C_6N_2H_{14}][Co_2(HPO_4)_3]$*

The synthesis of cobalt phosphate, **II**, was effected by reacting DABCO-phosphate with cobalt chloride in a predominantly nonaqueous medium. Thus, 0.238 g of

TABLE 3
Crystallographic Parameters of Open-Framework Metal Phosphates Synthesized from Amine Phosphates

Composition	Cell parameters						Sp. grp.	Ref.
	a (Å)	*b* (Å)	*c* (Å)	α (°)	β (°)	γ (°)		
				PIPP				
$[C_4N_2H_{12}][Zn(HPO_4)_2(H_2O)]$	8.931	14.025	9.311	90.0	95.4	90.0	$P2_1/n$	New
$[C_4N_2H_{12}][Zn_{3.5}(PO_4)_3(H_2O)]$	16.105	8.256	22.998	90.0	104.0	90.0	$C2/c$	New
$[C_4N_2H_{12}][Zn(H_2O)Zn(HPO_4)(PO_4)]_2$	12.076	14.889	11.836	90.0	97.7	90.0	$C2/c$	[10]
$[C_4N_2H_{12}][Zn_2(PO_4)(H_2PO_4)_2]$	13.388	12.839	8.225	90.0	94.8	90.0	$C2/c$	[10]
$[C_4N_2H_{12}][Zn_2(HPO_4)_2(H_2PO_4)_2]$[a]	13.414	12.871	8.225	90.0	94.8	90.0	$C2/c$	New
$[C_4N_2H_{12}]_{1.5}[Co(HPO_4)_2(PO_4)]H_2O$	8.388	8.576	23.899	90.0	93.9	90.0	$P2_1/c$	New
$[C_4N_2H_{12}]_{1.5}[Co(HPO_4)_2(PO_4)]H_2O$	8.169	26.340	8.385	90.0	93.9	90.0	$P2_1/c$	New
$[C_4N_2H_{12}]_{0.5}[Sn(PO_4)]$	9.063	7.810	10.067	90.0	115.3	90.0	$P2_1/c$	New
				DAP				
$[C_3N_2H_{12}][Zn(HPO_4)_2]$	5.220	12.756	15.674	90.0	90.0	90.0	$P2_12_12_1$	[11]
$[C_3N_2H_{12}][Zn_2(HPO_4)_3]$	8.615	9.619	17.038	90.0	93.6	90.0	$P2_1/c$	New
$[C_3N_2H_{12}][Co(HPO_4)_2]$	5.244	12.777	15.626	90.0	90.0	90.0	$P2_12_12_1$	[12]
$[C_3N_2H_{12}][Co_6Al_6(PO_4)_{12}(OH)_2]H_2O$	19.214	9.771	16.366	90.0	110.3	90.0	$P2_1/c$	New
$[C_3N_2H_{12}][SnPO_4]_2$	18.097	7.889	9.151	90.0	111.8	90.0	$C2/c$	[13]
				ENP				
$[C_2N_2H_{10}][Zn(HPO_4)_2]$	5.161	15.842	12.027	90.0	92.4	90.0	$P2_1/c$	[14]
$[C_2N_2H_{10}][Zn_2(HPO_4)_2(H_2PO_4)_2]$	16.420	7.826	14.640	90.0	116.5	90.0	$P2_1/c$	[14]
$[C_2N_2H_{10}][Zn_6(PO_4)_4(HPO_4)]$	19.182	5.036	21.202	90.0	103.3	90.0	$C2/c$	[15]
$[C_2N_2H_{10}]_{0.5}[Co(PO_4)]$	10.420	10.420	8.956	90.0	90.0	90.0	$P4_2/n$	New
$[C_2N_2H_{10}]_2[Co_4(PO_4)_2(HPO_4)_2]H_2O$	10.277	10.302	18.836	90.0	90.0	90.0	$P2_12_12_1$	New
$[C_2N_2H_{10}]_{0.5}[Co(PO_4)]$	14.719	14.734	17.891	90.0	90.02	90.0	$I2/b$	[16]
				DETAP				
$[C_4N_3H_{16}][Zn_4(PO_4)_3(HPO_4)]H_2O$	10.021	8.286	11.856	90.0	103.1	90.0	$P2_1$	[17]
$[C_4N_3H_{15}][Zn_2PO_4(HPO_4)]_2$	20.075	5.127	17.726	90.0	125.4	90.0	$C2/c$	[18]
$[C_4N_3H_{15}][Zn_5(PO_4)_4]$	27.071	5.215	17.920	90.0	130.3	90.0	Cc	[19]
$[C_2N_2H_{10}][Co_{3.5}(PO_4)_3]$[b]	5.080	15.203	16.354	90.0	95.7	90.0	$P2_1/n$	New
$[C_4N_3H_{15}]_{3.0}[Co_6(HPO_4)_3(PO_4)_5]$	31.950	8.360	15.920	90.0	96.6	90.0	$P2_1/c$	New
$[C_2N_2H_{10}]_{0.5}[Co(PO_4)]$[b]	10.420	10.420	8.956	90.0	90.0	90.0	$P4_2/n$	New
$[C_2N_2H_{10}]_{2.0}[Co_4(PO_4)_2(HPO_4)_2]H_2O$	10.277	10.302	18.836	90.0	90.0	90.0	$P2_12_12_1$	New
				DABCO-P				
$[C_6N_2H_{14}][Zn_2(HPO_4)_3]$	9.528	9.948	9.996	107.7	98.1	114.9	$P(-1)$	[20]
$[C_6N_2H_{14}][Zn_4(PO_4)_2(HPO_4)_2]3H_2O$	9.475	9.525	12.312	93.7	91.0	98.7	$P(-1)$	[20]
$[C_6N_2H_{14}][Co_2(HPO_4)_3]$[a]	9.552	9.980	10.001	107.7	97.9	114.9	$P(-1)$	New
				MPIP-P				
$[C_4N_2H_{12}][Zn_2(HPO_4)_2(H_2PO_4)_2]$[a]	13.414	12.871	8.225	90.0	94.8	90.0	$C2/c$	New
$[C_4N_2H_{12}]_{1.5}[Co(HPO_4)_2(PO_4)]H_2O$	8.388	8.576	23.899	90.0	94.0	90.0	$P2_1/c$	New
				APIP-P				
$[C_{10}N_4H_{26}]_{0.5}[Co(PO_4)Cl]$[a]	11.484	8.724	10.012	90.0	111.4	90.0	$P2_1/c$	New
				TMED-P				
$[C_6N_2H_{18}][Zn(H_2PO_4)_2(HPO_4)]$[a]	8.627	8.895	12.674	88.9	75.2	63.1	$P(-1)$	[26]

[a] Described in this work.
[b] Product of decomposition of the amine.

$CoCl_2 \cdot 6H_2O$ was dispersed in 4.6 ml of butan-2-ol. DABCO-phosphate (0.42 g) was added to the above under stirring. The mixture homogenized for about 15 min, transferred onto a 23-ml PTFE-lined stainless steel autoclave, and heated at 180°C for 48 h. The resultant product contained large quantities of deep blue crystals, were filtered under vacuum, washed with deionized water, and dried at ambient temperature.

TABLE 4
Crystal Data and Structure Refinement Parameters for the New Amine Phosphates

	MPIP-P	DABCO-P	APPIP-P	TMED-P
Empirical formula	$C_{10}H_{36}N_4O_{11}P_2$	$C_6N_2H_{17}O_5P_1$	$C_{10}H_{31}N_4O_6P_1$	$C_6H_{23}N_2O_6P_1$
M	450.4	228.2	334.3	250.3
Size (μm^3)	$40 \times 40 \times 120$	$120 \times 120 \times 240$	$120 \times 120 \times 200$	$120 \times 160 \times 240$
a (Å)	12.162(7)	6.906(2)	6.607(8)	8.209(4)
b (Å)	6.776(4)	9.018(4)	8.571(3)	8.411(6)
c (Å)	25.740(0)	9.271(2)	10.130(0)	8.617(6)
α (°)	90.00	92.2(1)	112.3(4)	114.2(9)
β (°)	103.2(9)	104.5(1)	96.5(6)	94.9(0)
γ (°)	90.00	111.7(6)	102.5(6)	118.0(4)
V (Å^3)	2064.6(3)	513.5(3)	504.4(7)	448.9(4)
Space group	$P2_1/n$	$P(-1)$	$P(-1)$	$P(-1)$
Z	4	2	2	2
2θ range (°)	46.54	46.54	46.60	46.58
No. of reflections	8172	2176	2158	1914
Unique data	2971	1448	1443	1273
Observed data [$I > 2\sigma(I)$]	1783	1397	1287	839
No of parameters	218	136	136	117
R_1	0.17[a]	0.04	0.05	0.07
wR_2	—	0.10	0.17	0.20
GOF	1.064	1.107	1.123	1.046

[a] Refined isotropically due to disorder of the amine molecules.

2.4. Synthesis of Cobalt Chlorophosphate, **III**, *$[C_{10}N_4H_{28}]_{0.5}[Co(PO_4)Cl]$*

The synthesis of cobalt chlorophosphate, **III**, was carried out by the reaction between cobalt chloride and 1,4-bis(3-aminopropyl)piperazine phosphate (APPIP-P) in butan-2-ol. $CoCl_2 \cdot 6H_2O$ (0.238 g) was dissolved in 4.6 ml of butan-2-ol and 0.596 g of APPIP-P was added under constant stirring. The mixture homogenized for 30 min was transferred onto a PTFE-lined stainless steel autoclave and heated at 160°C for 90 h. The resultant product contained large quantities of blue-colored plate-like crystals, was filtered

TABLE 5
Crystal Data and Structure Refinement Parameters for Compounds 1–V

	I	II	III	IV	V
Empirical Formula	$Zn_2P_4O_{16}C_4N_2H_{18}$	$Co_2P_3O_{12}C_6N_2H_{17}$	$CoPO_4ClC_5N_2H_{13}$	$ZnP_3O_{12}C_6N_2H_{23}$	$Zn_3P_4O_{20}C_6N_2H_{30}$
M	604.7	519.9	290.4	473.4	770.1
a (Å)	13.414(3)	9.551(6)	11.484(1)	8.627(2)	8.953(9)
b (Å)	12.871(2)	9.979(7)	8.723(9)	8.894(9)	9.712(9)
c (Å)	8.225(1)	10.000(8)	11.011(7)	12.674(2)	13.533(7)
α (°)	90.00	107.67(5)	90.00	88.94(3)	90.00
β (°)	94.78(0)	97.92(7)	111.37(5)	75.17(0)	95.98(6)
γ (°)	90.00	114.91(3)	90.00	63.06(5)	90.00
V (Å^3)	1415.2(2)	783.8(4)	1027.3(3)	832.8(2)	1170.5(9)
Space group	$C2/c$	$P(-1)$	$P2_1/c$	$P(-1)$	$P2_1/c$
Z	4	2	4	2	4
2θ range (°)	3–46.52	3–46.58	3–46.42	3–46.48	3–46.52
Total reflections	2908	3315	4153	3555	4801
Unique data	1018	2213	1459	2369	1679
Observed data [$I > 2\sigma(I)$]	918	2162	1340	2346	1343
No of parameters	106	226	127	218	177
R_1	0.03	0.04	0.03	0.05	0.03
wR_2	0.07	0.11	0.08	0.13	0.09
GOF	1.053	1.113	1.053	1.085	1.098

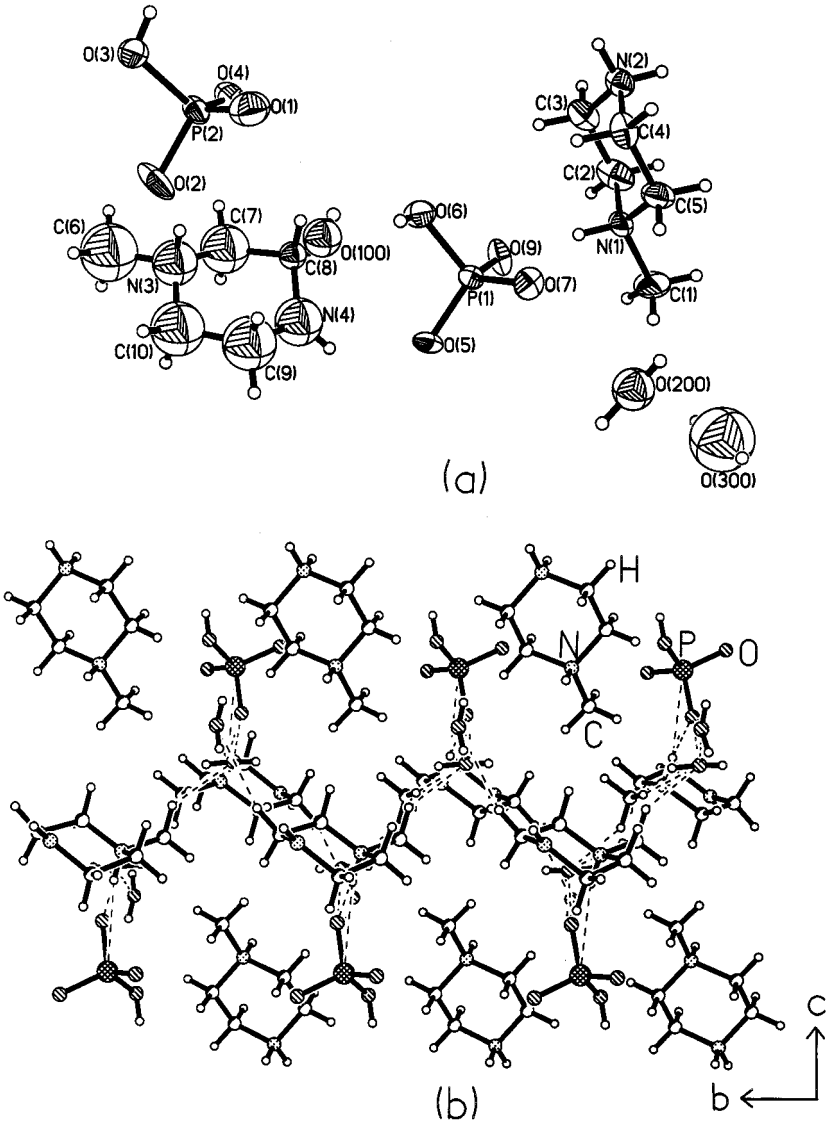

FIG. 1. (a) ORTEP plot of the structure of MPIP-P. Thermal ellipsoids are given at 50% probability. (b) Structure showing the hydrogen bond assembly between the HPO_4, diprotanated amine molecules, and water molecules. Dotted lines represent hydrogen bond interactions.

under vacuum, washed with deionized water, and dried at ambient temperature. To our knowledge, this is the first open-framework chlorophosphate to be reported in the literature.

2.5. Synthesis of Zinc Phosphate, **IV**, *$[C_6N_2H_{18}][Zn(H_2PO_4)_2(HPO_4)]$*

A mixture of 1 mmol of $ZnSO_4 \cdot 7H_2O$ dissolved in 10 mmol of H_2O and 2 mmol of TMED-P was stirred to obtain a homogeneous gel. The gel was left at room temperature (298 K) for about 1 week, to obtain large quantities of colorless crystals of the Zn phosphate, **IV**. The crystals were filtered under vacuum and washed with deionized water and dried at room temperature. **IV** could also be obtained by the reaction of the zinc salt, amine, and H_3PO_4 at room temperature for an extended period of time.

2.6. Synthesis of Zinc Phosphate, **V**, *$[C_6N_2H_{18}][Zn_3(H_2O)_4(HPO_4)_4]$*

The synthesis of zinc phosphate, **V**, was carried out by reacting 25 mM of the dried crystals of **IV** in 10 mM of water and heating in a PTFE-lined stainless steel autoclave at 50°C for 2 days. The resultant plate-like single crystalline product was filtered, washed with water, and dried at room temperature.

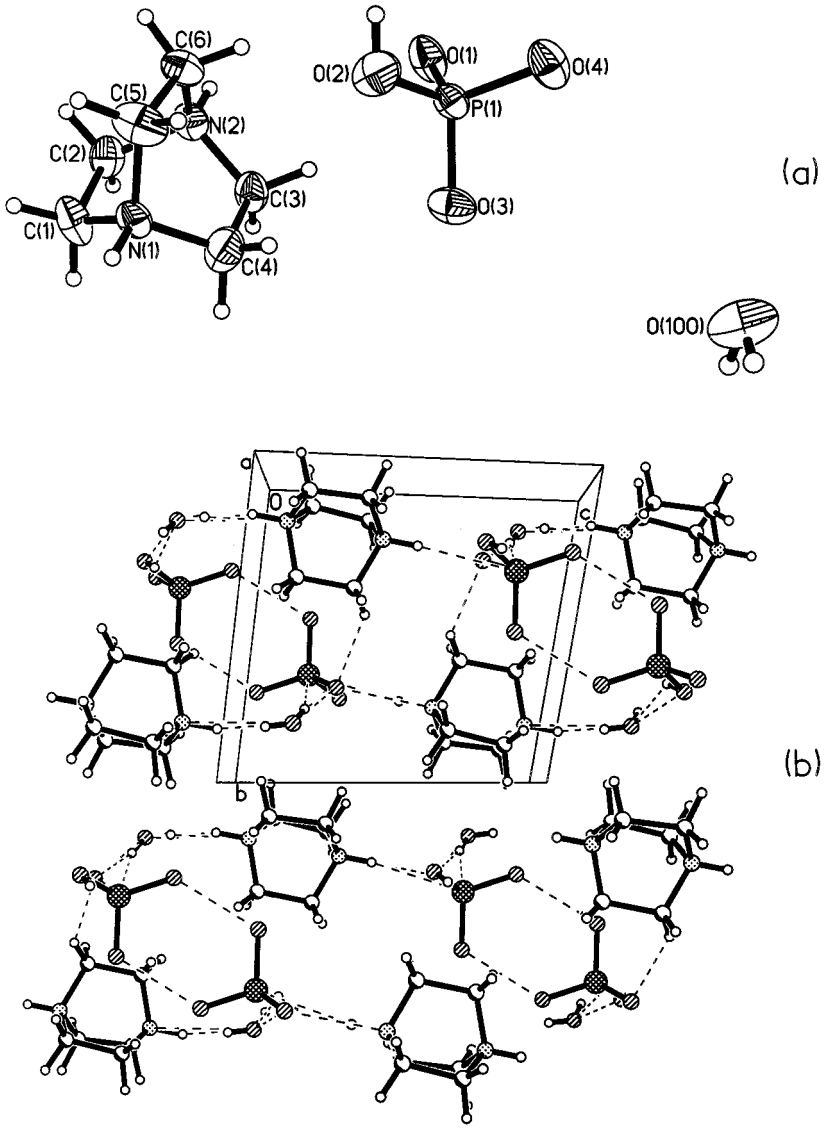

FIG. 2. (a) ORTEP plot of the structure of DABCO-P. Thermal ellipsoids are given at 50% probability. (b) Structure showing the layer-like hydrogen bond assembly between the HPO_4, diprotanated amine molecules and water molecules. Dotted lines represent the various hydrogen bond interactions.

2.7. Single Crystal Structure Determination

The crystal structures of the amine phosphates were determined by single crystal X-ray diffraction from a suitable single crystal. Data collection was performed on Siemens SMART diffractometer with a CCD detector. The structure was solved by SHELXS-86 (21) and refined using the SHELXTL-PLUS (22) suit of programs. The relevant details of the single crystal structure determination of some of the new amine phosphates are presented in Table 4. A similar procedure was adopted in the structure determination of metal phosphates. The structures were solved by direct methods using SHELXS-86 (21), which readily established the heavy atom (M, P) sites and most of the light atom (O, N, C) positions. All the hydrogen positions were located from difference Fourier maps and for the final refinement the hydrogens were placed geometrically and held in the riding mode. We discuss the structures of a few of the new open-framework metal phosphates, **I–V**, in this paper to demonstrate the efficacy as well as the versatility of amine phosphates in yielding these materials. The relevant details of the structure determination of the metal phosphates, **I–V**, are presented in Table 5. The last cycles of refinements included atomic coordinates, anisotropic thermal

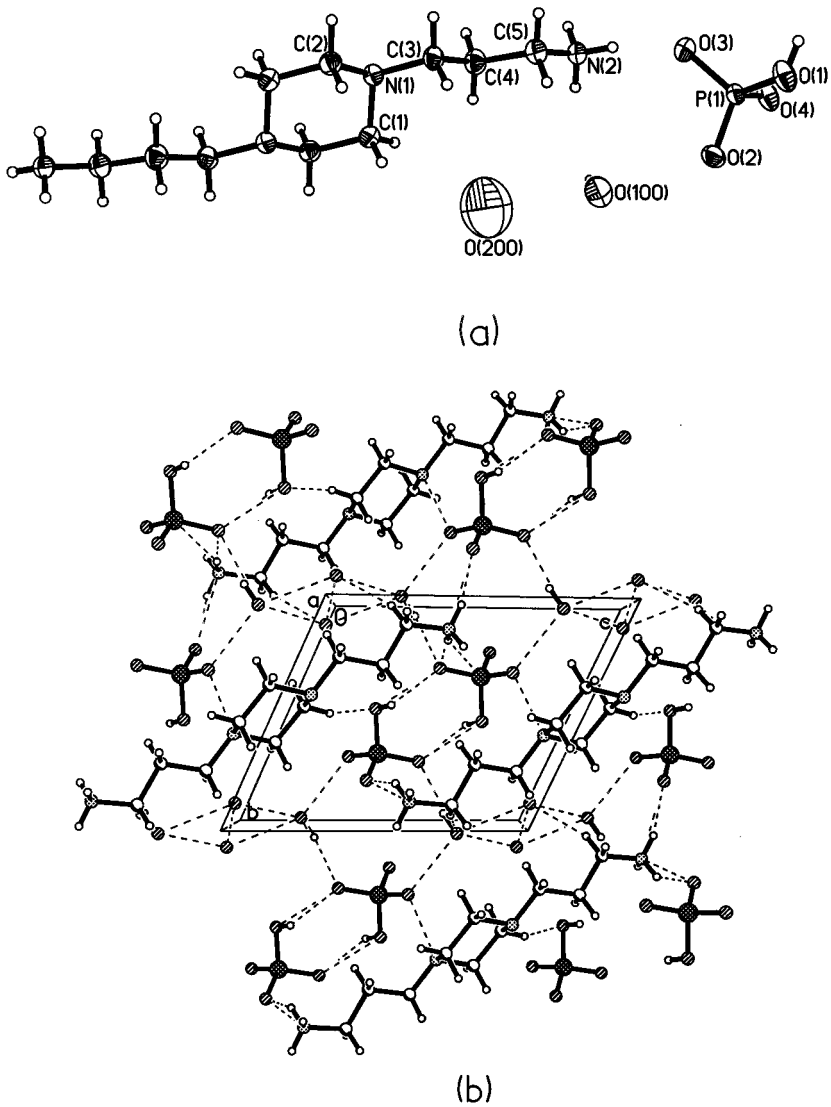

FIG. 3. (a) ORTEP plot of the structure of APIP-P. Thermal ellipsoids are given at 50% probability. (b) Structure showing the hydrogen bond assembly between the HPO_4, diprotanated amine molecules, and water molecules. Dotted lines represent hydrogen bonding.

parameters for all the nonhydrogen atoms and isotropic thermal parameters for all the hydrogen atoms. Full-matrix least-squares refinement on $|F^2|$ were carried out using the program SHELXTL-PLUS (22).

3. RESULTS

3.1. Structures of Amine Phosphates

The asymmetric unit of MPIP-P is presented in Fig. 1a. The structure of this amine phosphate comprises a hydrogen-bonded network of HPO_4 and doubly protonated *n*-methylpiperazine units. There is one molecule of HPO_4 and one molecule of *n*-methylpiperazine making this compound to be a 1 : 1 adduct. The structure also contains two molecules of water of hydration, which also actively participates in hydrogen bonding. The extended hydrogen-bonded network between the various units resembles a sheet-like architecture as shown in Fig. 1b.

The asymmetric unit of DABCO-P is given in Fig. 2a. The structure consists of a 1 : 1 adduct of HPO_4 and doubly protonated DABCO molecules with one molecule of water of hydration. The structure forms a sheet with alternating phosphorus and amine molecules linked via the water molecules as shown in Fig. 2b.

The asymmetric unit of APPIP-P shown in Fig. 3a, consists of one HPO_4 molecule and half a molecule of the

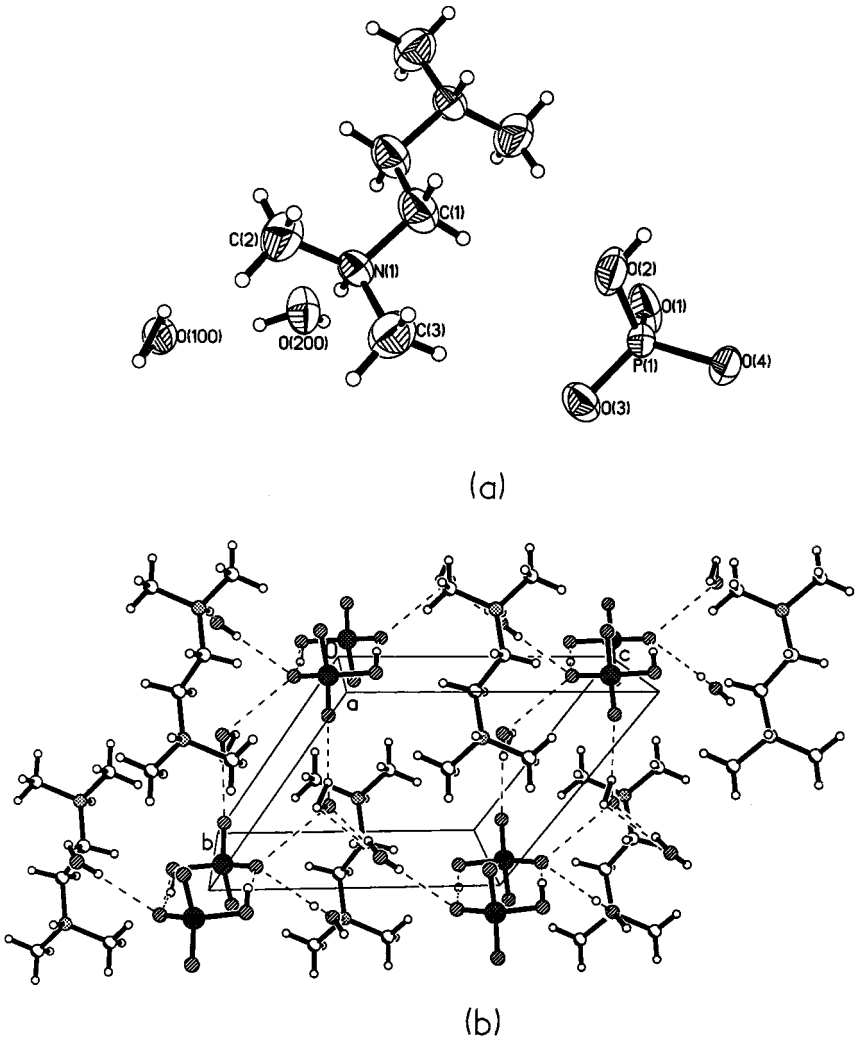

FIG. 4. (a) ORTEP plot of the structure of TMED-P. Thermal ellipsoids are given at 50% probability. (b) Structure showing the hydrogen bond assembly between the HPO_4, diprotanated amine molecules, and water molecules. Dotted lines represent hydrogen bond interactions.

diprotonated amine. The sheet-like architecture of APPIP-P contains two phosphate units on either side of the amine molecule as shown in Fig. 3b. The water molecules are situated between the amine molecules. The structure of TMED-P involves one amine and one HPO_4 unit as shown in Fig. 4a. The structure is arranged in such a way that the amine and HPO_4 units alternate along the *ab* plane forming a sheet (Fig. 4b).

3.2. Structure of $[C_4N_2H_{12}]_{0.5}[Zn(HPO_4)(H_2PO_4)]$, **I**

The atomic coordinates for **I** are presented in Table 6. The asymmetric unit of **I**, shown in Fig. 5a, consists of 12 independent nonhydrogen atoms. The structure of **I** is based on a three-dimensional network involving ZnO_4, $PO_3(OH)$, and $PO_2(OH)_2$ tetrahedra forming an anionic framework. Charge compensation is achieved by the incorporation of the double protonated piperazinium cation. With $0.5[C_4N_2H_{12}]^{2+}$ per framework formula unit. The piperazinium cation results from the demethylation of the MPIP-P under the reaction conditions. Such a decomposition of amine molecules during hydrothermal synthesis is well-documented (23). The framework is made from infinite corner-shared linear chains comprising of four-memberd rings running perpendicular to one another (Fig. 5b). At the junction of two such chains, the chains connect up in such a way that they go out of plane in different directions (Fig. 5b). While one chain connects in the downward direction of the plane, the other connects upward creating the three-dimensional connectivity (Fig. 5c). Four such

TABLE 6
Atomic Coordinates [$\times 10^4$] and Equivalent Isotropic Displacement Parameters [$Å^2 \times 10^3$] for I, $[C_4N_2H_{12}]_{0.5}[Zn(HPO_4)(H_2PO_4)]$

Atom	*x*	*y*	*z*	*U*(eq)[a]
Zn(1)	3794(1)	6217(1)	393(1)	13(1)
P(1)	1415(1)	6293(1)	−982(1)	14(1)
P(2)	5000	5409(1)	−2500	11(1)
O(1)	4868(2)	6119(2)	−1023(3)	17(1)
O(2)	4055(2)	5253(2)	2176(3)	20(1)
O(3)	2504(2)	6043(2)	−756(4)	34(1)
O(4)	3809(2)	7589(2)	1462(3)	22(1)
O(5)	918(2)	5557(2)	−2291(3)	24(1)
O(6)	889(2)	6131(2)	639(4)	36(1)
N(1)	6529(2)	7080(2)	280(3)	21(1)
C(1)	7444(2)	6410(3)	373(4)	24(1)
C(2)	6629(3)	7967(3)	−843(4)	26(1)

[a] *U*(eq) is defined as one-third of the trace of the orthogonalized U_{ij} tensor.

junctions make a 16-membered *clover* like aperture with each point where such a junction occurs creates a terminal of a *clove* (Fig. 6). The –OH groups of the HPO_4 unit protrude into this aperture. These apertures (channels) are reminiscent of the gallophosphate-"cloverite," which has similar 20-membered channels where fluoride ions extend into the channel (24).

The various geometrical parameters listed in Table 7 are in the range expected for this type of structure. Typically, the Zn–O distances are in the range 1.915–1.973 Å and the O–Zn–O bond angles are in the range 104.1–113.5° which clearly indicates that zinc atoms are in tetrahedral environment. The zinc atoms are connected to P atoms via oxygen atoms. The P–O distances are in the range 1.492–1.574 Å, and the O–P–O bond angles are in the range 104.7–114.1°. Bond valence-sum calculations (25) indicate the valence states of Zn, P, and O to be +2, +5, and −2, respectively, in agreement with the formula derived from single crystal structure determination.

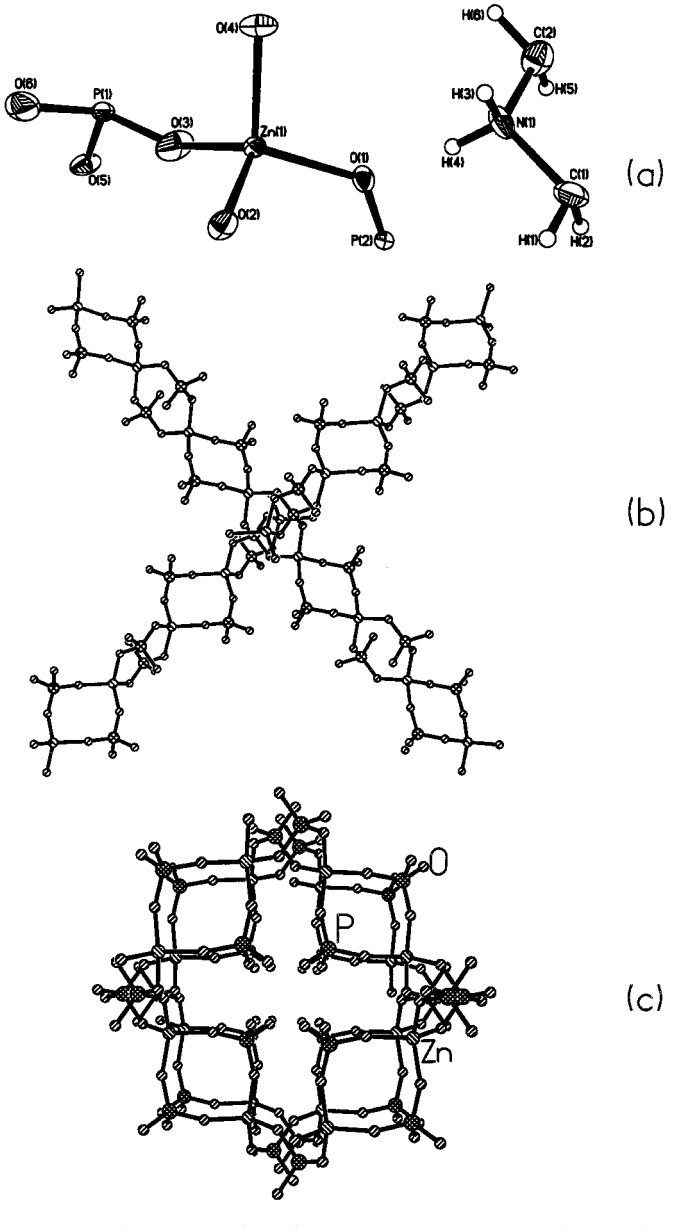

FIG. 5. (a) ORTEP plot of **I**, $[C_4N_2H_{12}]_{0.5}[Zn(HPO_4)(H_2PO_4)]$. Thermal ellipsoids are given at 50% probability. (b) Cross-linking of corner-shared 4-membered chains. (c) Structure of a single 16-membered clover-like channel in **I**, formed by the linkages between the corner-shared chains.

3.3. *Structure of $[C_6N_2H_{14}][Co_2(HPO_4)_3]$],* **II**

$[C_6N_2H_{14}][Co_2(HPO_4)_3]$, **II**, is a new three-dimensional open-framework structure containing one-dimensional channels bound by 8-*T* atoms (*T* = Co and P). The atomic coordinates of **II** are listed in Table 8. The 25 nonhydrogen atoms of the asymmetric unit consist of 17 framework and 8 atoms of the guest species, respectively (Fig. 7a). The two independent cobalt atoms in **II** are both tetrahedrally coordinated by their O atom neighbors with average cobalt–oxygen bond distances of 1.951 Å for Co(1) and 1.950 Å for Co(2). The P atoms, make three P–O–Co bonds and the remaining is a terminal P–O bond. The P–O bond distances are in the range 1.504–1.592 Å [$(P(1)–O)_{av.} = 1.537$, $(P(2)–O)_{av.} = 1.538$, $(P(3)–O)_{av.} = 1.536$ Å], and the O–P–O angles are the range 104.8°–115.2° [$(O–P(1)–O)_{av.} = 109.5°$, $(O–P(2)–O)_{av.} = 109.4°$, $(O–P(3)–O)_{av.} = 109.4°$]. These values are in good agreement with those observed in other open-framework phosphates (26–30). The P–O distances, P(1)–O(10), P(2)–O(11), and P(3)–O(12) of 1.590, 1.592, and 1.590 Å, respectively, are P–OH moieties. Thus, all the phosphorus units in **II** are actually HPO_4 units. The presence of terminal –OH groups attached to the

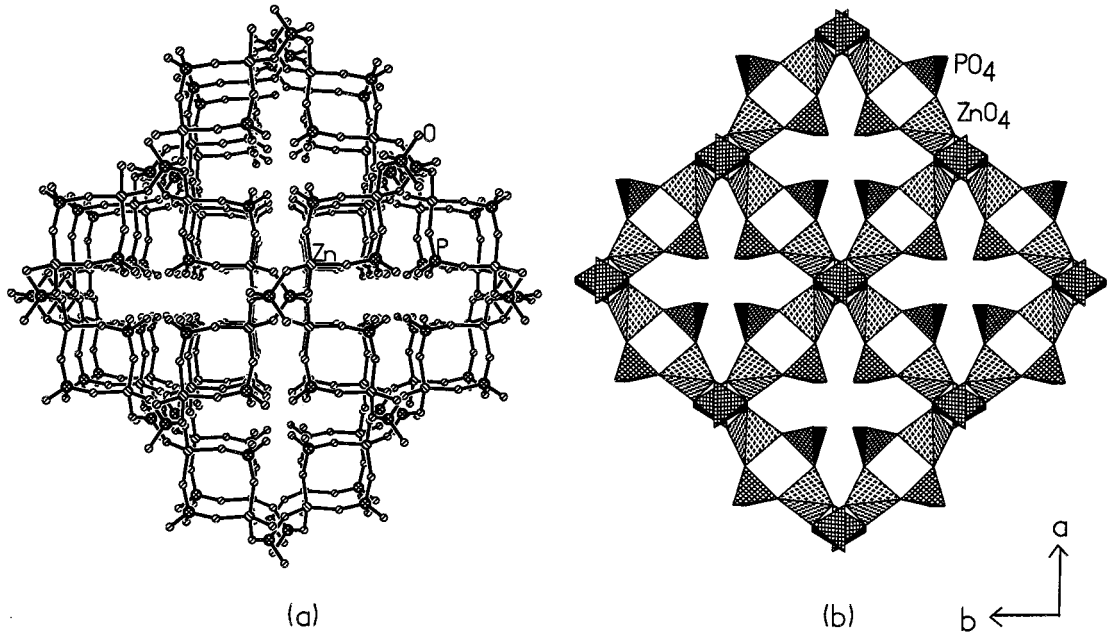

FIG. 6. Structure of **I**, $[C_4N_2H_{12}]_{0.5}[Zn(HPO_4)(H_2PO_4)]$ along the *c* axis showing the clover-like 16-membred channels. Amine molecules are omitted for clarity. (a) Ball–stick structure and (b) polyhedral structure.

P atoms is consistent with the bond-valence sum calculations (25).

The framework structure of **II** is built up from CoO_4 and $PO_3(OH)$ tetrahedra sharing vertices forming four-membered rings. The three-dimensional structure can be considered to be made from two-dimensional sheets formed by Co(1), Co(2), P(2), and P(3) and are connected by the third phosphate [P(1)] units. Within each sheet, there are two different types of four-membered rings; one made by Co(1) and P(3) and the other by Co(2) and P(2). These four-membered rings are linked via oxygen atoms forming eight-membred distorted pore openings within the layer. These sheets are connected by P(1) units forming one-dimensional channels bound by 8-*T* atoms (*T* = Co and P) as shown in Fig. 7b. The channels are formed along the *bc* plane and the width is $\sim 3.6 \times 4.8$ Å (the longest atom–atom contact distance not including the van der Waals radii). Along the *ac* direction there is another eight-membered channels formed by the linkages between the tetrahedra. The –OH groups of the $PO_3(OH)$ tetrahedra protrude into this channels. The doubly protonated DABCO molecules are located in the eight-ring channels.

3.4. Structure of the Chlorophosphate, $[C_{10}N_4H_{28}]_{0.5}[Co(PO_4)Cl]$, **III**

The atomic coordinates of the cobalt chlorophosphate, **III**, are presented in Table 9. The asymmetric unit of $[C_{10}N_4H_{28}]_{0.5}[Co(PO_4)Cl]$, shown in Fig. 8, consists of 14 nonhydrogen atoms. There is only one crystallographically independent cobalt and phosphorus atom in the asymmetric unit. Phosphorus is coordinated by four oxygen atoms, whereas, cobalt is coordinated by three oxygens and one chlorine atom. Though cobalt and phosphorus are tetrahedrally coordinated with respect to the nearest atom neighbors, they are only three Co–O–P bonds. The remaining connection needed for the tetrahedral linkage comes from a terminal bonding of a chlorine with cobalt (Co(1)–Cl(1) = 2.291 Å) and for phosphorus from a double bonded oxygen atom (P(1)–O(4) = 1.538 Å). Bond valence sum calculations (25) on the framework also agree with the above formulations. The Co–O and P–O bond distances as well as the O–Co–O and O–P–O angles are in the expected range for this type of bonding (Table 10).

The layered framework structure of $[C_{10}N_4H_{28}]_{0.5}[Co(PO_4)Cl]$, is built up from a network of CoO_3Cl and PO_4 tetrahedra sharing vertices. The vertex-shared linkages between these tetrahedron gives rise to a two-dimensional macroanionic layer with four- and eight-membered apertures within each layer as shown in Fig. 9. The chlorine atoms, bonded to cobalt atoms, point in a direction perpendicular to the plane of the layer. This arrangement of the chlorine atoms facilitates closer interaction with the structure-directing amines via Cl....H–N/C-type interaction. The compensating cationic structure-directing amine molecule, 1,3-*bis* aminopropyl

TABLE 7
Selected Bond Distances and Angles for I, $[C_4N_2H_{12}]_{0.5}[Zn(HPO_4)(H_2PO_4)]$

Moiety	Distance (Å)	Moiety	Angle (°)
Zn(1)–O(3)	1.915(2)	O(2)–Zn(1)–O(4)	104.04(9)
Zn(1)–O(1)	1.931(2)	O(3)–P(1)–O(4)[a]	114.05(14)
Zn(1)–O(2)	1.931(2)	O(3)–P(1)–O(5)	108.45(14)
Zn(1)–O(4)	1.973(2)	O(4)[a]–P(1)–O(5)	109.66(13)
P(1)–O(3)	1.492(2)	O(3)–P(1)–O(6)	111.6(2)
P(1)–O(4)[a]	1.516(2)	O(4)[b]–P(1)–O(6)	104.66(13)
P(1)–O(5)	1.543(2)	O(5)–P(1)–O(6)	108.2(2)
P(1)–O(6)	1.574(3)	O(2)[b]–P(2)–O(2)[c]	112.5(2)
P(2)–O(2)[b]	1.532(2)	O(2)[b]–P(2)–O(1)	108.58(11)
P(2)–O(2)[c]	1.532(2)	O(2)[c]–P(2)–O(1)	109.88(11)
P(2)–O(1)	1.542(2)	O(2)[b]–P(2)–O(1)[d]	109.88(11)
P(2)–O(1)[d]	1.542(2)	O(2)[c]–P(2)–O(1)[d]	108.58(11)
		O(1)[a]–P(2)–O(1)[d]	107.3(2)
	Angle (°)	P(2)–O(1)–Zn(1)	130.88(13)
O(3)–Zn(1)–O(1)	112.55(11)	P(2)[c]–O(2)–Zn(1)	125.74(13)
O(3)–Zn(1)–O(2)	113.54(11)	P(1)–O(3)–Zn(1)	150.7(2)
O(1)–Zn(1)–O(2)	108.63(9)	P(1)[a]–O(4)–Zn(1)	137.7(2)
O(3)–Zn(1)–O(4)	107.41(10)		
O(1)–Zn(1)–O(4)	110.32(9)		
	Organic moiety Distance (Å)		
N(1)–C(1)	1.486(6)	C(1)–N(1)–C(4)	111.0(3)
N(1)–C(4)	1.495(6)	C(3)–N(2)–C(2)	111.5(4)
N(2)–C(3)	1.492(6)	N(1)–C(1)–C(2)	110.8(4)
N(2)–C(2)	1.493(6)	N(2)–C(2)–C(1)	111.3(4)
C(1)–C(2)	1.525(7)	N(2)–C(3)–C(4)	110.7(4)
C(3)–C(4)	1.511(7)	N(1)–C(4)–C(3)	110.3(4)
N(3)–C(5)	1.486(6)	C(5)–N(3)–C(6)	110.8(4)
N(3)–C(6)	1.489(6)	N(3)–C(5)–C(6)[d]	110.2(4)
C(5)–C(6)[d]	1.507(7)	N(3)–C(6)–C(5)[d]	109.1(4)

Note. Symmetry transformations used to generate equivalent atoms: [a] $x, -y+3/2, z-1/2$. [b] $x, -y+3/2, z+1/2$. [c] $-x+1, -y+1, -z$. [d] $-x, -y+1, -z+1$.

TABLE 8
Atomic Coordinates [× 10^4] and Equivalent Isotropic Displacement Parameters [$Å^2$ × 10^3] for II, $[C_6N_2H_{14}][Co_2(HPO_4)_3]$

Atom	x	y	z	U(eq)[a]
Co(1)	−3144(1)	12066(1)	1567(1)	12(1)
Co(2)	−1362(1)	10330(1)	6126(1)	12(1)
P(1)	1749(1)	14007(1)	7300(1)	13(1)
P(2)	−1558(1)	10292(1)	3063(1)	14(1)
P(3)	−3369(1)	9695(1)	8385(1)	13(1)
O(1)	−3412(4)	11094(3)	9492(3)	28(1)
O(2)	−1770(4)	11592(3)	2757(3)	26(1)
O(3)	1710(3)	15587(3)	7892(3)	20(1)
O(4)	−4908(3)	8108(3)	7966(3)	24(1)
O(5)	−2495(3)	9646(3)	4038(3)	24(1)
O(6)	65(3)	12640(3)	6982(3)	20(1)
O(7)	−3062(3)	9996(3)	7032(3)	19(1)
O(8)	−262(3)	9069(3)	6258(3)	18(1)
O(9)	3043(3)	13956(3)	8320(3)	22(1)
O(10)	2190(4)	13844(3)	5803(3)	27(1)
O(11)	−2191(3)	8822(3)	1513(3)	21(1)
O(12)	−1869(3)	9546(4)	9083(3)	25(1)
N(1)	−8487(4)	5199(4)	2469(3)	19(1)
N(2)	−5594(4)	5996(4)	2703(4)	21(1)
C(6)	−6599(6)	4208(5)	1955(6)	33(1)
C(5)	−8316(6)	3717(5)	2005(5)	27(1)
C(4)	−7474(5)	6289(5)	4042(5)	27(1)
C(3)	−5746(6)	6559(6)	4197(5)	33(1)
C(2)	−6126(5)	6753(5)	1813(5)	28(1)
C(1)	−7954(5)	6056(5)	1488(4)	22(1)

[a] U(eq) is defined as one-third of the trace of the orthogonalized $U_{I,j}$ tensor.

piperazine, is situated in between these inorganic layers as shown in Figs. 10 and 11. Thus, $[C_{10}N_4H_{28}]_{0.5}[Co(PO_4)Cl]$, is a typical example of a two-dimensional structure possessing alternating inorganic and organic layers.

3.5. *Structure of the Monomeric Zinc Phosphate, $[C_6N_2H_{18}][Zn(H_2PO_4)_2(HPO_4)]$,* **IV**

The structure of **IV** consists of four-membered rings formed by ZnO_4 and $PO_2(OH)_2$ tetrahedra with $PO_3(OH)$ and $PO_2(OH)_2$ moieties hanging from the Zn center as shown in Fig. 12 (26). These monomeric zinc phosphate moiety is stabilized by extensive intramolecular multipoint hydrogen bonding involving the phosphate units as well as the doubly protonated amine molecule, forming a sheet-like structure. The bond distances and angles in **IV** are presented in Table 11.

3.6. *Structure of $[C_6N_2H_{18}][Zn_3(H_2O)_4(HPO_4)_4]$,* **V**

As mentioned earlier, compound **V** was obtained by heating **IV** (the zinc phosphate monomer) in water at 50°C for 2 days. The structure of **V** comprises a network of $Zn(1)O_4$, $Zn(2)O_2(H_2O)_4$, and $PO_3(OH)$ moieties, in which the vertices are shared (26). The linkages between these units give rise to a layered architecture. The connectivity between these units forms a bifurcated eight-membered aperture within the layers as shown in Fig. 13. Bifurcated layers have been observed earlier in open-framework zinc phosphates (14). It is interesting to note that Zn(2) links only with the two P(1) atoms and the remaining Zn–O linkages are terminal water which are pointed into the aperture and interacts with the framework via hydrogen bonding. As is typical of layered structures, the structure-directing amine molecule is situated in between the layers. The doubly protonated amine molecule interacts with the framework via multipoint hydrogen bonding and is partly responsible for the observa-

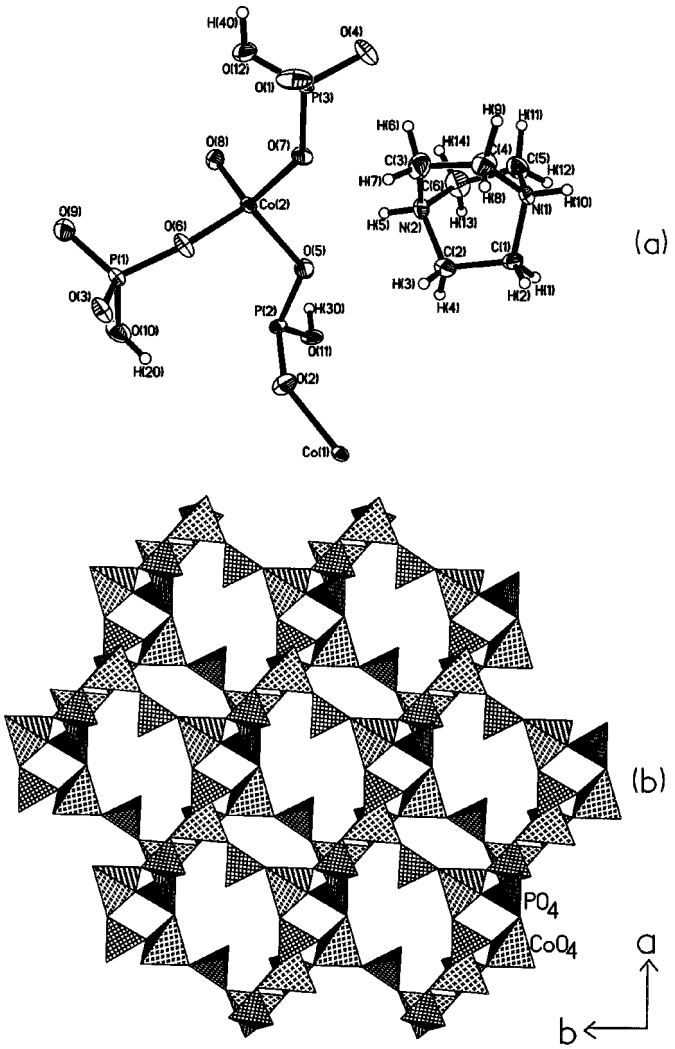

FIG. 7. (a) ORTEP plot of **II**, $[C_6N_2H_{14}][Co_2(HPO_4)_3]$. Thermal ellipsoids are given at 50% probability.(b) Polyhedral structure of **II** along the *bc* direction showing the eight-membred channels.

tion of such an architecture. Selected bond distances and angles in **V** are presented in Table 12.

4. DISCUSSION

Six new amine phosphates have been synthesized in the present study. They generally show layer/tape-like architectures involving hydrogen bond interactions. The N…O and O…O distances in the amine phosphates are all generally around 2.6 Å and the N–H…O and O–H…O bond angles are all $> 150°$. Clearly, the N–H…O bonds in these materials is strong. It is interesting that the amine : phosphoric acid ratio is 1 : 1 in all these compounds, and the protons are transferred by the acid to the amine giving rise to the quarternary ammonium species. This situation is ideal for the synthesis of metal phosphates, as in most cases the framework is anionic and the charge compensation is achieved through the protonated organic amines.

TABLE 9
Atomic coordinates [$\times 10^4$] and Equivalent Isotropic Displacement Parameters [$Å^2 \times 10^3$] for, III, $[C_{10}N_4H_{28}]_{0.5}[Co(PO_4)Cl]$

Atom	*x*	*y*	*z*	U_{eq}[a]
Co(1)	1441(1)	977(1)	6924(1)	13(1)
P(1)	−1041(1)	−1243(1)	6050(1)	12(1)
Cl(1)	3427(1)	−2(1)	7771(1)	22(1)
O(1)	1448(2)	2583(2)	8162(2)	23(1)
O(2)	285(2)	−685(2)	6892(2)	24(1)
O(3)	1003(2)	1983(2)	5210(2)	20(1)
O(4)	−1966(2)	107(2)	5679(2)	19(1)
N(1)	1136(2)	6930(3)	4407(2)	19(1)
C(1)	2026(3)	5729(3)	5158(3)	24(1)
C(2)	2472(3)	5991(3)	6610(3)	23(1)
C(3)	3452(3)	4778(3)	7279(3)	18(1)
N(2)	3966(2)	4919(2)	8733(2)	15(1)
C(4)	4757(3)	3558(3)	9339(3)	18(1)
C(5)	4728(3)	6338(3)	9194(3)	18(1)

[a] U_{eq} is defined as one-third of the trace of the orthogonalized U_{ij} tensor.

TABLE 10
Selected Bond Distances and Angles in $[C_{10}N_4H_{28}]_{0.5}[Co(PO_4)Cl]$

Moiety	Distance (Å)	Moiety	Distance (Å)
Co(1)–O(1)	1.952(2)	P(1)–O(1)[a]	1.522(2)
Co(1)–O(2)	1.957(2)	P(1)–O(2)	1.544(2)
Co(1)–O(3)	1.973(2)	P(1)–O(3)[b]	1.546(2)
Co(1)–Cl(1)	2.291(1)	P(1)–O(4)	1.538(2)
	Organic Moiety		
N(1)–C(1)	1.487(4)	C(1)–C(2)	1.507(5)
C(2)–C(3)	1.525(4)	C(3)–N(2)	1.496(4)
N(2)–C(4)	1.497(4)	N(2)–C(5)	1.494(4)
	Angle (°)	Moiety	Angle (°)
O(1)–Co(1)–O(2)	112.0(1)	O(1)[a]–P(1)–O(2)	108.1(1)
O(1)–Co(1)–O(3)	106.5(1)	O(1)[a]–P(1)–O(3)[b]	110.2(1)
O(2)–Co(1)–O(3)	112.2(1)	O(2)–P(1)–O(3)[b]	109.1(1)
O(1)–Co(1)–Cl(1)	103.5(1)	O(1)[a]–P(1)–O(4)	109.9(1)
O(2)–Co(1)–Cl(1)	107.4(1)	O(2)–P(1)–O(4)	110.7(1)
O(3)–Co(1)–Cl(1)	115.1(1)	O(3)[b]–P(1)–O(4)	108.9(1)
	Organic Moiety		
N(1)–C(1)–C(2)	112.5(2)	C(1)–C(2)–C(3)	108.2(2)
C(2)–C(3)–N(2)	113.2(2)	C(3)–N(2)–C(4)	110.5(2)
C(3)–N(2)–C(5)	112.7(2)	C(4)–N(2)–C(5)	108.7(2)
N(2)–C(4)–C(5)[c]	111.6(2)	N(2)–C(5)–C(4)[c]	111.5(2)

Note. Symmetry transformations used to generate equivalent atoms: [a] $-x, y-1/2, -z+3/2$; [b] $-x, -y, -z+1$; [c] $-x+1, -y+1, -z+2$.

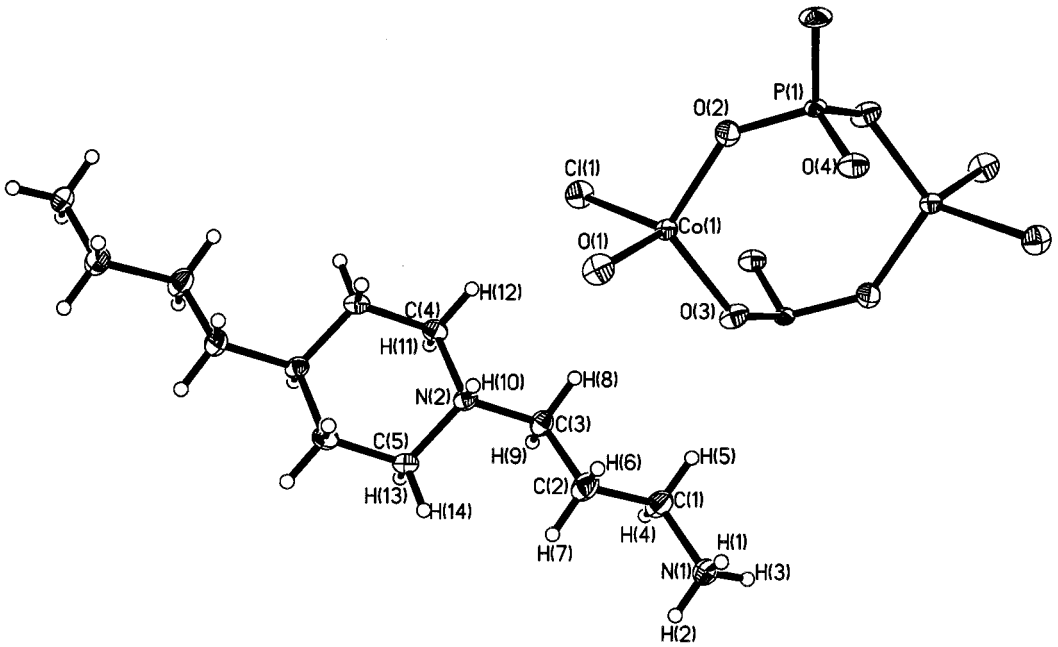

FIG. 8. ORTEP plot of **III**, $[C_{10}N_4H_{28}]_{0.5}[Co(PO_4)Cl]$. Thermal ellipsoids are given at 50% probability.

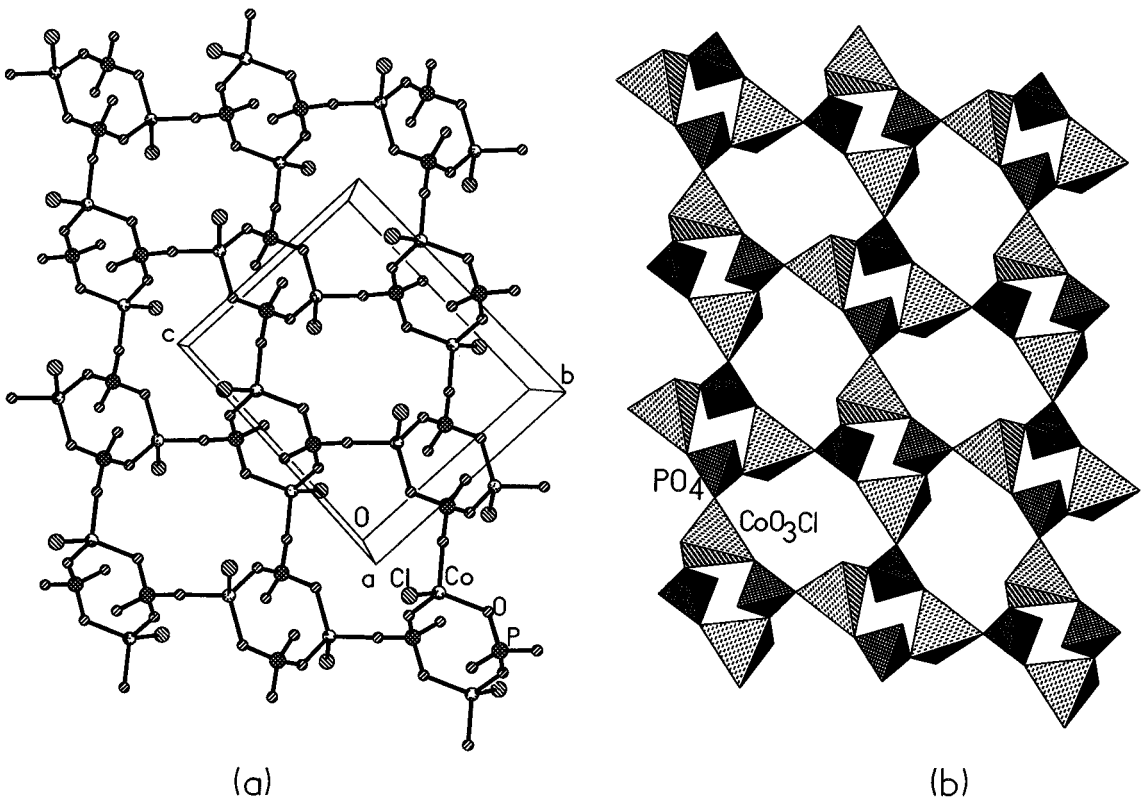

FIG. 9. Structure of **III**, along the *a* axis showing a single layer. Note that the layers are made of four- and eight-membred rings only. (a) Ball and stick view, (b) polyhedral view.

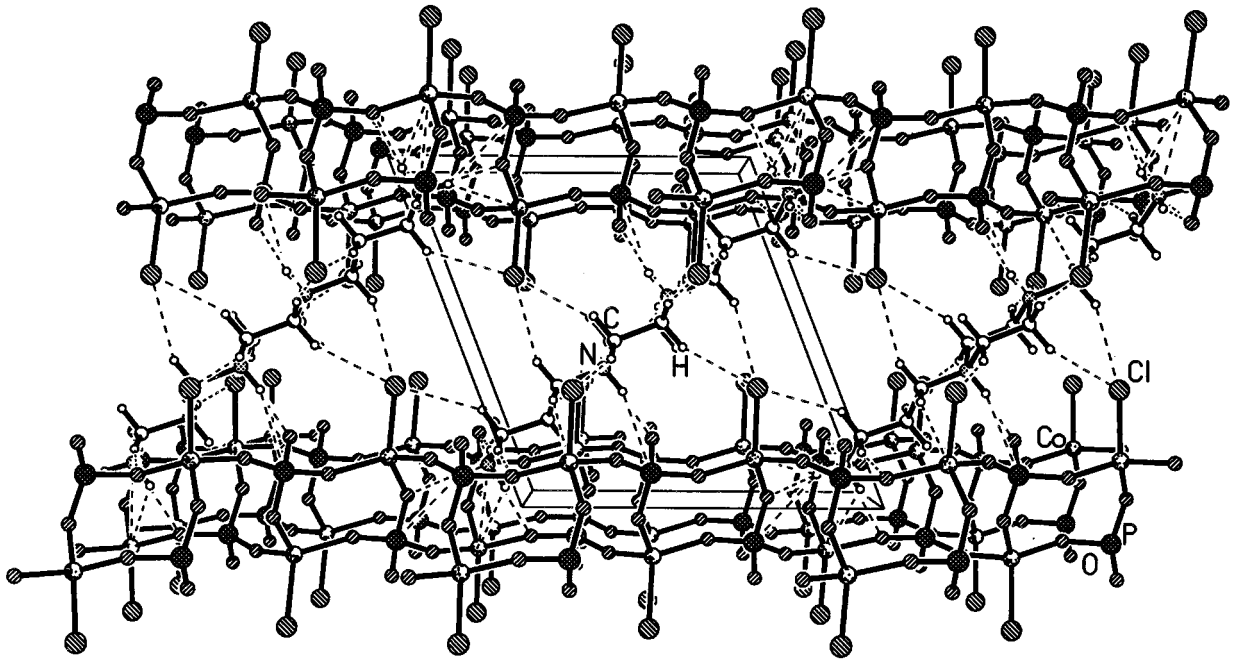

FIG. 10. Structure of **III**, along the *b* axis showing the inorganic layers and the amine in between. Note that the chlorine atoms point into the interlamellar space.

Additionally, the amine phosphates act as *in situ* source of both the amine and the phosphorus. The large number and variety of open-framework materials, derived from the amine phosphates indicate their seminal role as likely intermediates in the formation of open structures. Of the six new amine phosphates reported in the present study, we have used four of them for the synthesis of open-framework metal phosphates. It is noteworthy that the amine phosphates

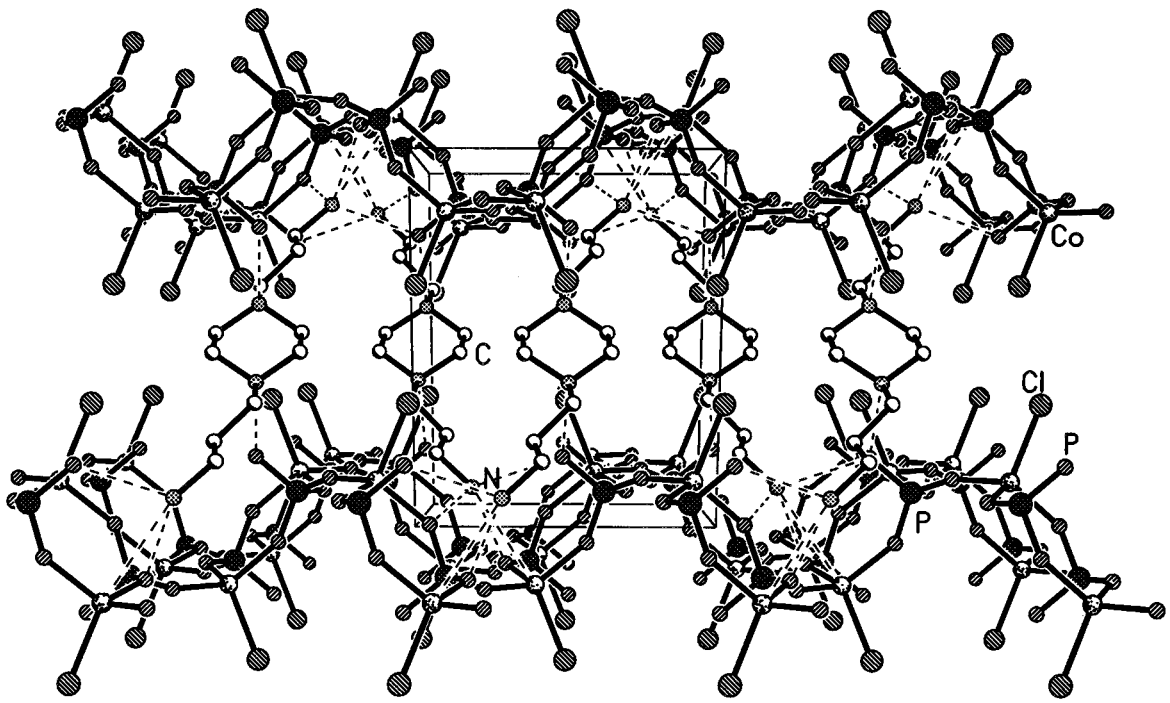

FIG. 11. Structure of **III**, along the *c* axis showing the layers and the amine molecules. Dotted lines represent the various hydrogen bond interactions observed in **III**.

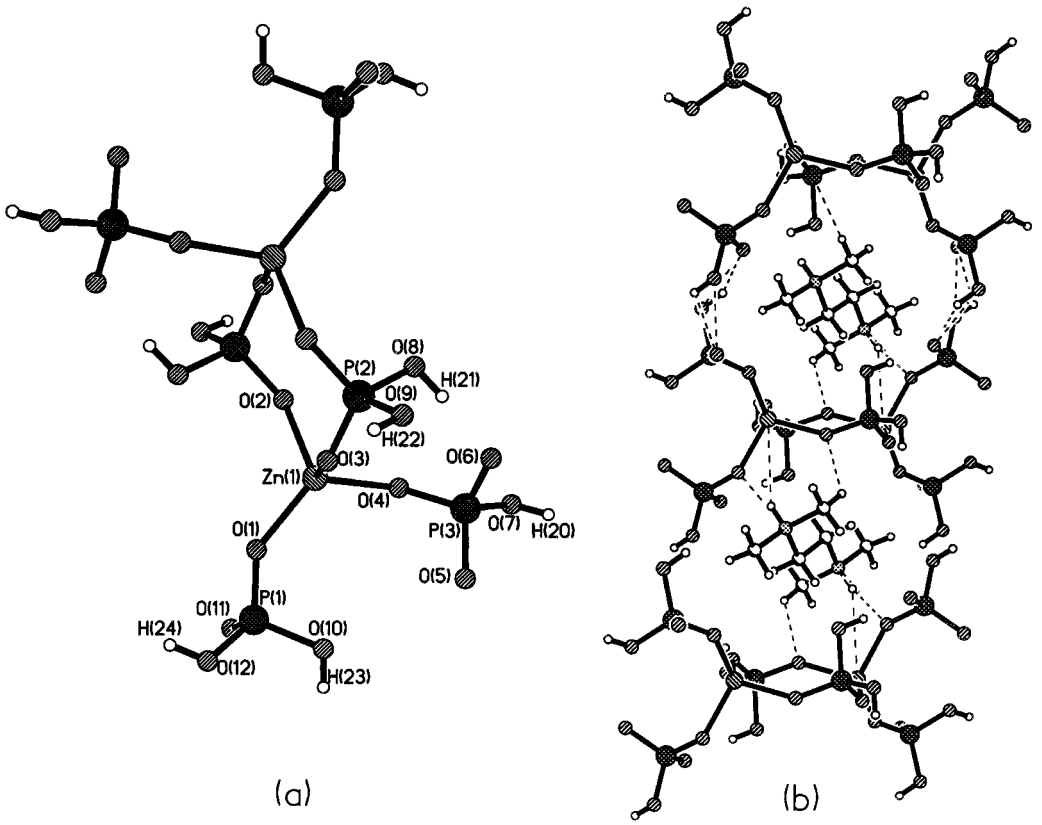

FIG. 12. Hydrogen bonded assembly of **IV** and the amine. The sheet-like architecture has cavities where the amine molecules reside. Dotted lines represent hydrogen-bond interactions.

react with metal ions well below the temperatures normally employed in hydrothermal synthesis (150–200°C). Thus, the reactions of PIPP and other amine phosphates with Zn^{2+} and Co^{2+} ions give the open-framework structures at considerably lower temperatures (50–90°C). This observation corroborates the role of the amine phosphates as reaction intermediates. The formation of a metal phosphate from an amine phosphate could indeed be a simple substitution reaction as shown in Fig. 14. The likely role of the amine phosphate as a reaction intermediate facilitating the reaction with metal ions to yield an open architectures provides a useful handle for fine tuning the formation of newer structures with a better control than normally possible. Such a control has enabled us to obtain three interesting structures: a zinc phosphate, **I**, with a clover-like structure, **III**, an open-framework chlorophosphate, and **IV**, a zinc phosphate monomer involving a four-membered ring, which constitutes the basic building block of open-framework structures.

The chlorophosphate, **III**, is the first of its kind reported in the literature, wherein the chlorine of the starting metal chloride is retained in the open-framework phosphate as well. In most instances, the chlorine of the starting metal chloride is eliminated during the formation of the metal phosphate (17–19) and the role of Cl^- is similar to that of F^- ions reported in the literature (27). In **III**, the use of the amine phosphate probably facilitated the incorporation of the chlorine into the framework. It is instructive to compare the role of the chlorine atoms in **III** with that of the lone-pair of electrons of Sn(II) atoms in some of the tin(II) phosphates and oxalates (13, 23, 28–30). As can be seen from Figs. 9–11 the chlorine atoms in the chlorophosphate is projected perpendicular to the plane of the layer. Similar positioning has been observed for the lone pair of electrons in the tin phosphate and oxalates as shown in Fig. 15. In the tin(II) phosphates, the Sn atoms are usually coordinated with three oxygen atoms and occupy the vertex of a trigonal pyramid. The oxygens are, in turn, connected to phosphorus completing the tin phosphate structure. The fourth vertex needed for the tetrahedron, in the case of Sn(II), are provided by the lone pair of electrons. The stereo-active lone pairs manifest themselves in the lattice by creating open space between the two layers in these tin phosphates. In the present compounds, we have a similar situation with

TABLE 11
Selected Bond Distances and Angles for IV, $[C_6N_2H_{18}][Zn(H_2PO_4)(HPO_4)]$

Moiety	Distance (Å)	Moiety	Angle (°)
Zn(1)–O(1)	1.920(3)	O(3)–Zn(1)–O(4)	111.35(13)
Zn(1)–O(2)	1.947(3)	O(1)–P(1)–O(11)	114.0(2)
Zn(1)–O(3)	1.961(3)	O(1)–P(1)–O(10)	106.8(2)
Zn(1)–O(4)	1.973(3)	O(11)–P(1)–O(10)	112.6(2)
P(1)–O(1)	1.494(4)	O(1)–P(1)–O(12)	109.3(2)
P(1)–O(11)	1.515(3)	O(11)–P(1)–O(12)	109.1(2)
P(1)–O(10)	1.561(3)	O(10)–P(1)–O(12)	104.6(2)
P(1)–O(12)	1.573(3)	O(2)[a]–P(2)–O(3)	114.6(2)
P(2)–O(2)[a]	1.507(3)	O(2)[a]–P(2)–O(9)	109.7(2)
P(2)–O(3)	1.512(3)	O(3)–P(2)–O(9)	109.3(2)
P(2)–O(9)	1.568(3)	O(2)[a]–P(2)–O(8)	108.2(2)
P(2)–O(8)	1.570(3)	O(3)–P(2)–O(8)	110.5(2)
P(3)–O(5)	1.506(3)	O(9)–P(2)–O(8)	103.9(2)
P(3)–O(6)	1.531(3)	O(5)–P(3)–O(6)	112.2(2)
P(3)–O(4)	1.542(3)	O(5)–P(3)–O(4)	112.2(2)
P(3)–O(7)	1.588(3)	O(6)–P(3)–O(4)	110.5(2)
		O(5)–P(3)–O(7)	109.6(2)
	Angle (°)	O(6)–P(3)–O(7)	107.6(2)
		O(4)–P(3)–O(7)	104.4(2)
O(1)–Zn(1)–O(2)	111.3(2)	P(1)–O(1)–Zn(1)	143.4(2)
O(1)–Zn(1)–O(3)	111.17(14)	P(2)[a]–O(2)–Zn(1)	137.5(2)
O(2)–Zn(1)–O(3)	108.13(14)	P(2)–O(3)–Zn(1)	126.8(2)
O(1)–Zn(1)–O(4)	113.35(13)	P(3)–O(4)–Zn(1)	126.8(2)
O(2)–Zn(1)–O(4)	101.04(13)		
	Organic Moiety		
	Distance (Å)		
N(1)–C(2)	1.483(7)	C(2)–N(1)–C(3)	111.0(4)
N(1)–C(3)	1.498(7)	C(2)–N(1)–C(1)	117.4(4)
N(1)–C(1)	1.519(7)	C(3)–N(1)–C(1)	104.8(4)
C(1)–C(1)[b]	1.527(12)	N(1)–C(1)–C(1)[b]	109.5(6)
N(2)–C(4)	1.489(6)	C(4)–N(2)–C(5)	109.6(4)
N(2)–C(5)	1.504(6)	C(4)–N(2)–C(6)	113.3(4)
N(2)–C(6)	1.507(6)	C(5)–N(2)–C(6)	109.9(4)
C(4)–C(4)[c]	1.531(9)	N(2)–C(4)–C(4)[c]	111.5(5)

Note. Symmetry transformations used to generate eqivalent atoms: [a] $x, -y+3/2, z-1/2$; [b] $x, -y+3/2, z+1/2$; [c] $-x+1, -y+1, -z$; [d] $-x, -y+1, -z+1$

TABLE 12
Selected Bond Distances and Angles for V, $[C_6N_2H_{18}][Zn_3(H_2O)_4(HPO_4)_4]$

Moiety	Distance (Å)	Moiety	Angle (°)
Zn(1)–O(1)	1.930(3)	O(5)–Zn(2)–O(6)	95.6(2)
Zn(1)–O(2)	1.947(3)	O(5)[a]–Zn(2)–O(6)	84.4(2)
Zn(1)–O(3)	1.952(3)	O(6)[a]–Zn(2)–O(6)	180.0
Zn(1)–O(4)	1.953(3)	O(5)–Zn(2)–O(7)[a]	97.0(2)
Zn(2)–O(5)	1.989(3)	O(5)[a]–Zn(2)–O(7)[a]	83.0(2)
Zn(2)–O(5)[a]	1.989(3)	O(6)[a]–Zn(2)–O(7)[a]	89.4(2)
Zn(2)–O(6)[a]	2.126(4)	O(6)–Zn(2)–O(7)[a]	90.6(2)
Zn(2)–O(6)	2.126(4)	O(5)–Zn(2)–O(7)	83.0(2)
Zn(2)–O(7)[a]	2.212(4)	O(5)[a]–Zn(2)–O(7)	97.0(2)
Zn(2)–O(7)	2.212(4)	O(6)[a]–Zn(2)–O(7)	90.6(2)
P(1)–O(5)	1.509(3)	O(6)–Zn(2)–O(7)	89.4(2)
P(1)–O(1)[b]	1.519(4)	O(7)[a]–Zn(2)–O(7)	180.0
P(1)–O(2)	1.527(3)	O(5)–P(1)–O(1)[b]	113.9(2)
P(1)–O(8)	1.583(4)	O(5)–P(1)–O(2)	111.2(2)
P(2)–O(3)	1.521(3)	O(1)[b]–P(1)–O(2)	107.7(2)
P(2)–O(9)	1.522(3)	O(5)–P(1)–O(8)	105.5(2)
P(2)–O(4)[c]	1.529(3)	O(1)[b]–P(1)–O(8)	109.0(2)
P(2)–O(10)	1.569(3)	O(2)–P(1)–O(8)	109.5(2)
		O(3)–P(2)–O(9)	112.5(2)
	Angle (°)	O(3)–P(2)–O(4)[c]	111.9(2)
		O(9)–P(2)–O(4)[c]	109.9(2)
O(1)–Zn(1)–O(2)	103.85(14)	O(3)–P(2)–O(10)	103.3(2)
O(1)–Zn(1)–O(3)	108.9(2)	O(9)–P(2)–O(10)	109.3(2)
O(2)–Zn(1)–O(3)	120.25(14)	O(4)[c]–P(2)–O(10)	109.7(2)
O(1)–Zn(1)–O(4)	109.67(14)	P(1)[d]–O(1)–Zn(1)	128.0(2)
O(2)–Zn(1)–O(4)	106.6(2)	P(1)–O(2)–Zn(1)	120.0(2)
O(3)–Zn(1)–O(4)	107.31(14)	P(2)–O(3)–Zn(1)	128.8(2)
O(5)–Zn(2)–O(5)[a]	180.0	P(2)[c]–O(4)–Zn(1)	122.2(2)
O(5)–Zn(2)–O(6)[a]	84.4(2)	P(1)–O(5)–Zn(2)	141.7(2)
O(5)[a]–Zn(2)–O(6)[a]	95.6(2)		
	Organic Moiety		
	Distance (Å)		
N(1)–C(2)	1.491(7)	C(2)–N(1)–C(3)	109.8(4)
N(1)–C(3)	1.493(7)	C(2)–N(1)–C(1)	112.5(4)
N(1)–C(1)	1.499(7)	C(3)–N(1)–C(1)	109.7(4)
C(1)–C(1)[e]	1.514(11)	N(1)–C(1)–C(1)[e]	112.1(5)

Note. Symmetry transformations used to generate equivalent atoms: [a] $x, -y+3/2, z-1/2$; [b] $x, -y+3/2, z+1/2$; [c] $-x+1, -y+1, -z$; [d] $-x, -y+1, -z+1$.

three oxygen atoms that bond cobalt to the phosphorus forming the layer arrangement. Since Co is tetrahedrally coordinated, the fourth connection comes from the chlorine atoms which occupy a position identical to that of the lone pair of electrons of Sn(II).

The role of amine phosphates as intermediates in the formation of open-framework metal phosphates was pointed out earlier. It is gratifying that an amine phosphate (TMED-P) has yielded the monomeric zinc phosphate, **IV**, on reaction with Zn^{2+} ions. The compounds **IV** and **V**, are special in the sense that **IV** is the only known monomer of the zinc phosphate family containing only the four-membered ring and giving rise to **V** on mild heating. In Fig. 16, we give a plausible pathway for the formation of **V** from **IV**. As can be seen, the step involves the formation of a simple chain form the monomer unit before forming the layers. This pathway is somewhat analogous to that proposed by Oliver *et al.* (5) for the aluminophosphate framework solids. Oliver *et al.* (5), however, treated the linear chain with corner-shared four-membered rings to be the fundamental building unit. According to the scheme in Fig. 16, the monomer loses a phosphate to form a chain structure which after losing another phosphate adds on a $ZnO_2(H_2O)_4$ unit to give the layer architecture of **V**, as described by the

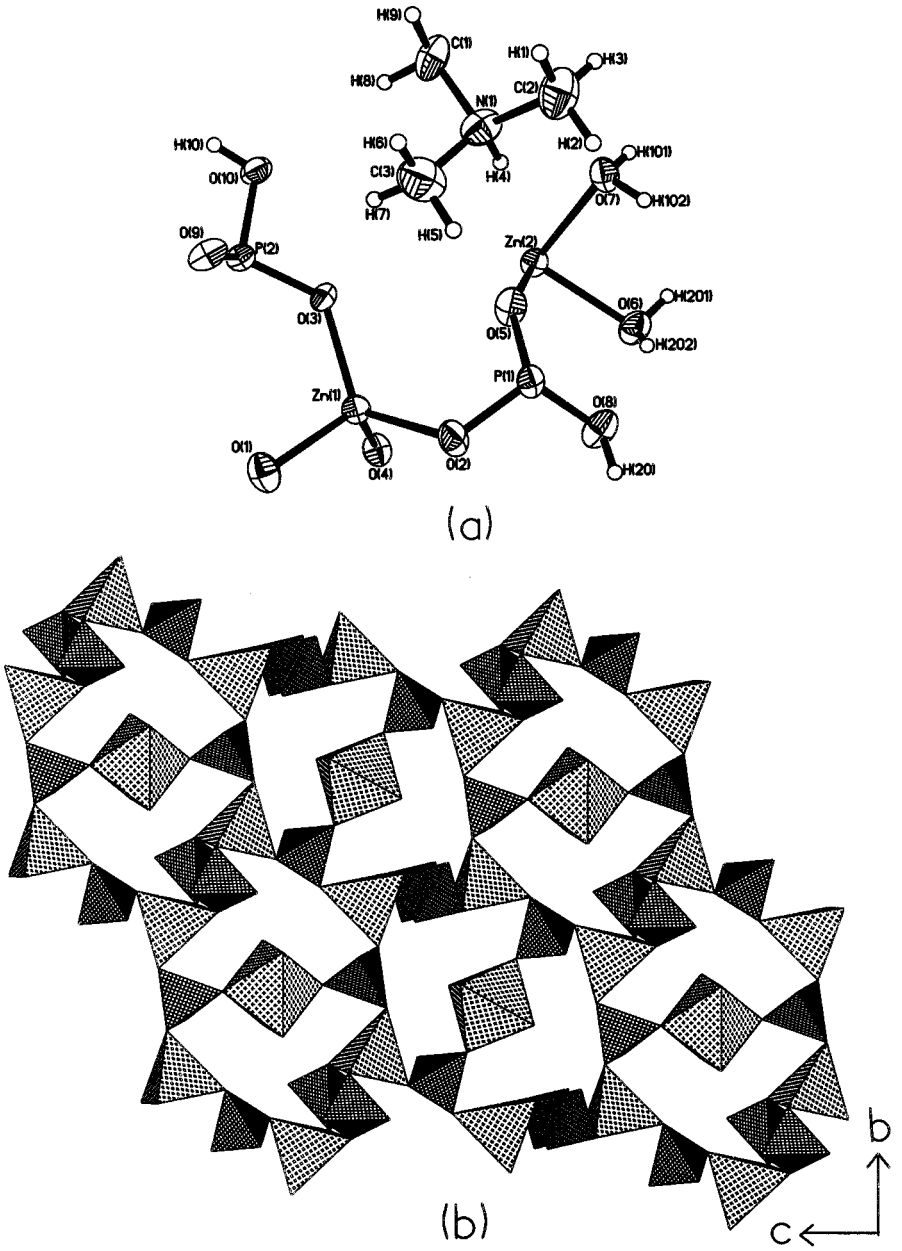

FIG. 13. (a) ORTEP plot of **V**, $[C_6N_2H_{18}][Zn_3(H_2O)_4(HPO_4)_4]$. Thermal ellipsoids are given at 50% probability. (b) Polyhedral view of the structure of **V** showing a single layer.

following reactions:

$$2[Zn(HPO_4)(H_2PO_4)_2] \xrightarrow{-H_2PO_4} [Zn_2(HPO_4)_2(H_2PO_4)_3]$$

$$\xrightarrow[+Zn]{-H_2PO_4} [Zn_3(HPO_4)_4].$$

The chain segments need only be sufficiently long to produce a secondary building unit (SBU) comprising the layer structure **V**, since the SBUs are likely to assemble spontaneously. Thus, the present study demonstrates how the amine phosphate route forms novel architecture including the monomeric phosphate. The monomeric phosphate containing the four-membered ring is likely to be the primary building block of open-framework metal phosphates.

It is interesting to ponder about the formation of complex open-framework structures from the primary or secondary building units. The mode of formation of open-framework

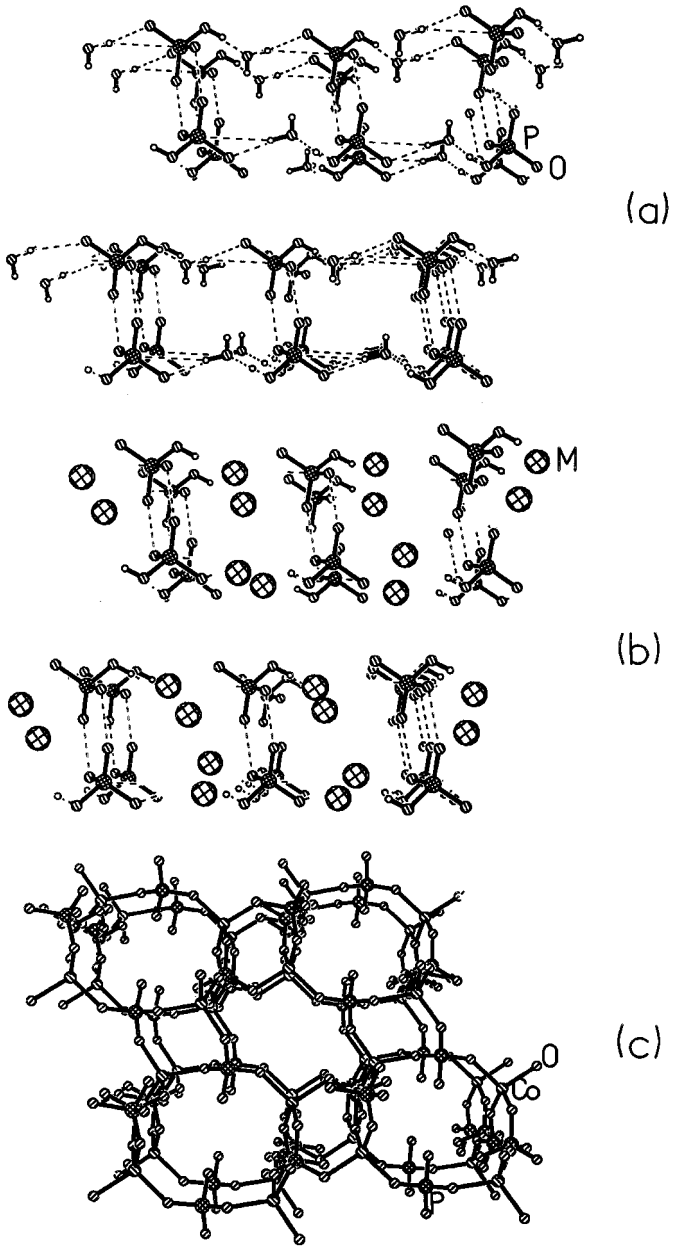

FIG. 14. Figure showing possible relation between the amine phosphate and the metal phosphate structures. (a) Structure of DABCO-P. Amine molecules have been omitted for clarity. Dotted lines represent hydrogen bond interactions. (b) Figure showing the metal atoms ($M = Co^{2+}$) replacing the water molecule in (a). (a) Structure of the cobalt phosphate $[C_6N_2H_{14}][Co_2(HPO_4)_3]$. Note that the replacement of water molecules by cobalt helps in the facile formation of this architecture.

structures from a linear chain involving corner-shared four-membered rings has been suggested by few workers (5, 31). It appears, however, that the primary reaction involves the formation of a unit such as the four-membered ring described here.

5. CONCLUSIONS

The present study demonstrates the seminal role of amine phosphates in the formation and synthesis of open-framework metal phosphates. That a large number and variety of metal phosphates could be made starting from the amine phosphates clearly demonstrates that the amine phosphates are likely to be the reaction intermediates in the hydrothermal synthesis of these open-framework materials. The synthesis of a metal phosphate monomer comprising only a four-membered ring and its subsequent condensation into a layered open-framework structure is vitally important for our understanding of the possible pathways involved in the formation of open architectures. It is equally important to carry out investigations to relate the open-framework structures obtained with the nature of the amines. While the present study has shown that the four-membered ring can give rise to open-framework structures, it would be worthwhile to investigate the condensation and or transformation of complex building units, such as the linear chain and ladder structures. The interaction between chains and ladders with a monomeric four-membered ring would also be of interest. The transformation of the linear chain to the ladder or layer structures probably involves hydrolysis, rotation, and condensation (5, 31) and it is likely that once such SBUs (chains and ladders) are formed the rest of the transformations are very facile as mentioned earlier. Further work is necessary to fully understand and exploit this amine phosphate route to design and control of the formation of open-framework structures.

An examination of the literature on the preponderance of the various open-framework structures shows the three-dimensional structures to be most common. While several ladder structures are known, there is one only linear chain structure reported hitherto (32). As mentioned earlier, the four-membered ring monomeric phosphate is equally rare. Thus, the frequency of occurrence of the different structures seems to be related to the nature of the open-framework structure. Since the low-dimensional structures as well as the four-membered ring are likely to be precursors of the complex three-dimensional structures, it is conceivable that they are difficult to isolate, considering that further assemblage of these units probably occurs spontaneously. It is also to be noted that the four-membered ring unit is isolated only when a complex amine is employed, but the linear chain is formed with a regular amine, such as piperazine. The isolation of the lower dimensional structures may in some way be related to the nature of the amine as well. There is reason to believe a tri- or a tetraamine might give rise to more open-framework structures than a simple mono- or diamine.

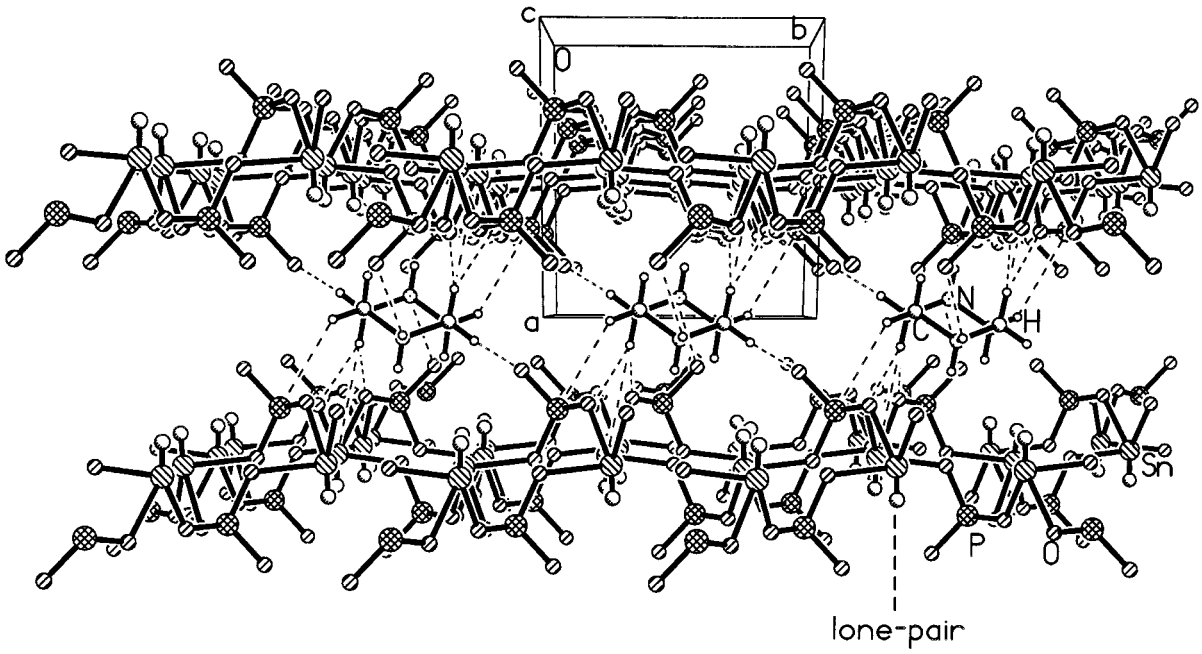

FIG. 15. Structure of the tin(II) phosphate, $[C_4N_2H_{12}]_{0.5}[Sn(PO_4)]$. Note that the lone pair of electrons point into the interlamellar region.

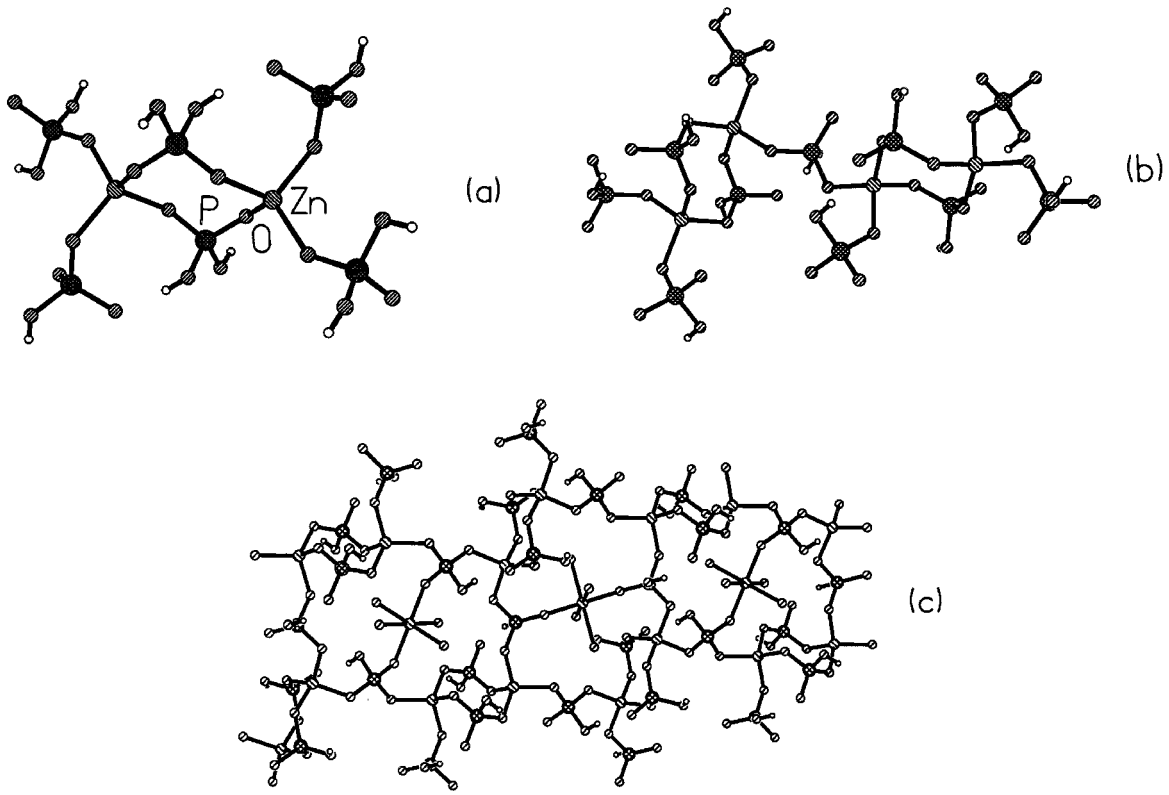

FIG. 16. (a) The zinc phosphate monomer, **IV**. (b) A possible chain-like architecture from the monomer by the elimination of a H_2PO_4 unit (see text). (b) Structure showing the layer arrangement of **V**, obtained by the elimination of a phosphate unit from (b), and the incorporation of a Zn octahedron.

REFERENCES

1. A. K. Cheetham, T. Loiseau, and G. Ferey, *Angew. Chem. Int. Ed.* **39,** 3268 (1999).
2. J. M. Thomas, *Angew. Chem. Int. Ed. Engl.* **33,** 913 (1994); *Chem. Eur. J.* **3,** 1557 (1997).
3. M. E. Davis and R. F. Lobo, *Chem. Mater.* **4,** 756 (1992).
4. G. Ferey, *C.R. Acad. Sci. Paris II* 1 (1998).
5. S. Oliver, A. Kuperman, A. Lough, and G. A. Ozin, *Chem. Mater.* **8,** 2391 (1996); S. Oliver, A. Kuperman, and G. A. Ozin, *Angew. Chem. Int. Ed. Engl.* **37,** 46 (1997).
6. S. Neeraj, S. Natarajan, and C. N. R. Rao, *Angew. Chem. Int. Ed.* **39,** 3480 (1999).
7. D. Riou, T. Loiseau, and G. Ferey, *Acta Crystallogr. Sect. C* **49,** 1237(1993).
8. S. Kamoun, A. Jouini, and A. Dasud, *Acta Crystallogr. Sect. C* **36,** 1481 (1980), also see **47,** 1481 (1991).
9. M. T. Averbuch-Pouchot and A. Durif, *Acta Crystallogr. Sect. C* **43,** 1894 (1987).
10. P. Feng, X. Bu, and G. D. Stucky, *Angew. Chem. Int. Ed. Engl.* **34**, 1745 (1995).
11. W. T. A. Harrison, Z. Bircsak, L. Hannooman, and Z. Zhang, *J. Solid State Chem.* **136,** 93 (1998).
12. A. M. Chippindale and A. R. Cowley, *J. Chem. Soc., Dalton Trans.* 2147 (1999).
13. R. Vaidhyanathan and S. Natararjan, *J. Mater. Chem.* **9,** 1807 (1999).
14. D. Chidambaram, S. Neeraj, S. Natarajan, and C. N. R. Rao, *J. Solid State Chem.* **147,** 154 (1999).
15. D. Chidambaram and S. Natarajan, *Mater. Res. Bull.* **33,** 1275 (1998).
16. J. Chen, R. H. Jones, S. Natarajan, M. B. Hursthouse, and J. M. Thomas, *Angew. Chem. Int. Ed. Engl.* **33,** 639 (1994).
17. S. Neeraj, S. Natarajan, and C. N. R. Rao, *Chem. Commun.* 165 (1999).
18. S. Neeraj, S. Natarajan, and C. N. R. Rao, *Chem. Mater.* **11,** 1390 (1999).
19. S. Neeraj, S. Natarajan, and C. N. R. Rao, *New J. Chem.* **23,** 303 (1999).
20. W. T. A. Harrison, T. E. Martin, T. E. Gier, and G. D. Stucky, *J. Mater. Chem.* **2,** 175 (1992).
21. G. M. Sheldrick, "SHELXS-86 Program for Crystal Structure Determination," Univ. of Göttingen, 1986; *Acta. Crystallogr. A* **35,** 467 (1990).
22. G. M. Sheldrick, "SHELXTL-PLUS Program for Crystal Structure Solution and Refinement," Univ. of Göttingen, 1993.
23. S. Natarajan, *J. Mater. Chem.* **8,** 2757 (1998), and references therein.
24. M. Esterman, L. B. McCusker, Ch. Baerlocher, A. Merrouche, and H. Kessler, *Nature* **352,** 320 (1991).
25. I. D. Brown and D. Altermatt, *Acta Crystallogr. Sect. B.* **41,** 244 (1984).
26. S. Neeraj, S. Natarajan, and C. N. R. Rao, *J. Solid State Chem.* **150,** 417 (2000).
27. A. M. Chippindale, S. Natarajan, J. M. Thomas, and R. H. Jones, *J. Solid State Chem.* **111,** 18 (1994); A. M. Chippindale, and C. Turner, *J. Solid State Chem.* **128,** 318 (1997).
28. S. Ayyappan, X. Bu, A. K. Cheetham, S. Natarajan, and C. N. R. Rao, *Chem. Commun.* 2181 (1998).
29. S. Ayyappan, A. K. Cheetham, S. Natarajan, and C. N. R. Rao, *Chem. Mater.* **10,** 3746 (1998)
30. S. Natarajan, R. Vaidhyanathan, C. N. R. Rao, S. Ayyappan, and A. K. Cheetham, *Chem. Mater.* **11,** 1633 (1999).
31. L. Vidal, C. Marichal, V. Gramlich, J. Patarin, and Z. Gabelica, *Chem. Mater.* **11,** 2728 (1999).
32. C. N. R. Rao, S. Natarajan, and S. Neeraj, *J. Am. Chem. Soc.* **122,** 2810 (2000).